

RESEARCH

Open Access



Polymerization of deoxygenated sickle hemoglobin in the presence of fractionated leaf extracts of *Anacardium occidentale*, *Psidium guajava*, and *Terminalia catappa*

Paul C. Chikezie^{*} , Raphael C. Ekeanyanwu and Adaeze B. Chile-Agada

Abstract

Background: The present study evaluated levels of polymerization of deoxygenated sickle hemoglobin molecules (poly-dHbS-M) in the presence of fractionated leaf extracts of *Anacardium occidentale* Linn., *Psidium guajava* Linn., and *Terminalia catappa* Linn in vitro as well as identified, quantified, and characterized the phytocomponents from fractionated leaf extracts that exhibited comparatively high potency to impede poly-dHbS-M. Non-hemolyzed sickle erythrocytes were premixed with 40, 60, and 80 mg/100 mL of each of the separate fractionated leaf extracts of *A. occidentale*, *P. guajava*, and *T. catappa* in phosphate-buffered saline (PBS; pH = 7.4), osmotically equivalent to 9.0 g/L NaCl. Poly-dHbS-M was induced by adding 2.0 g/100 mL Na₂S₂O₅ to the erythrocyte suspension. The absorbance of the erythrocyte suspension was measured at regular intervals of 30 s for 180 s. Identification, quantification, and characterization of phytocomponents from fractionated leaf extracts were carried out using GC-MS, FT-IR, and UV-visible systems protocols.

Results: The level of poly-dHbS-M of the control sample was significantly higher ($p < 0.05$) than those of the samples containing 40, 60, and 80 mg/100 mL ethylacetate extracts of *A. occidentale* at $t < 60$ s. The relative cumulative polymerization index (RCPI%) of dHbS-M in the presence of fractionated leaf extract of *A. occidentale* varied within a wide range of 3.8–59.4%. *A. occidentale* (petroleum ether and ethylacetate extracts), *P. guajava* (*n*-hexane, chloroform, and ethylacetate extracts), and *T. catappa* (ethylacetate extract) exhibited comparatively high potency to inhibit poly-dHbS-M.

Conclusion: The fractionated leaf extracts of *A. occidentale*, *P. guajava*, and *T. catappa* exhibited differential capacities to impede poly-dHbS-M. The combinations of aliphatic hydrocarbons, methylated esters, methylated fatty acids, aliphatic alcohols, D-erythro-sphinganine, aromatic derivatives, cycloalkanes, phthalates, isothiocyanates, aminated sugars, cyclo-alcohols, and nitro-compounds impeded poly-dHbS-M.

Keywords: Sickle hemoglobin, *Anacardium occidentale*, *Psidium guajava*, *Terminalia catappa*, Polymerization

* Correspondence: p_chikezie@yahoo.com
Department of Biochemistry, Imo State University, Owerri, Nigeria

Background

Hemoglobin, a tetrameric conjugate protein molecule, is an attractive model for the study of the structure/function relationship of macromolecules. The sickle hemoglobin (HbS) variant or sickle erythrocyte hemoglobinopathy ($\alpha_2\beta_2^s$) is caused by a point mutation affecting the coding sequence of β -globin gene, whereby thymine is replaced by adenine with the concomitant replacement of adenine by uracil in the triplet code (GAA or GAG codon \rightarrow GUA or GUG codon)—a partially acceptable missense mutation. The mutant gene elicits the substitution of hydrophilic glutamic acid at the β^6 globin position for hydrophobic valine; $\beta^{6\text{Glu}\rightarrow\text{Val}}$ (Rotter et al. 2005; Bianchi et al. 2009). Hydrophobic β^6 valine (Val-beta6) generates a 'sticky patch' on the β -globin chains of deoxygenated sickle hemoglobin molecules (dHbS-M) (Martins 1983; Rotter et al. 2005). The contact position on dHbS-M is such that the hydrophobic R-group of Val-beta6 appears to fit into a hydrophobic pocket constituted by β^{88} leucine (Leu-beta88), β^{85} phenylalanine (Phe-beta85), and β^{73} aspartic acid (Asp-beta73) residues on adjacent dHbS-M (Adachi et al. 1994; Ferrone et al. 2002; Dash et al. 2013). The hydrophobic interaction is stereospecific of Leu-beta88 side chain in the acceptor pocket regions on adjacent dHbS-M (Adachi et al. 1994). The hydrophilic R-group of β^6 glutamic acid (Glu-beta6) would not easily fit into the hydrophobic pocket explaining at least part of the reasons deoxyHbA does not polymerize (Martins 1983). The inter-hydrophobic interactions promote nucleation of dHbS-M followed by their alignment into microfibrils aggregations of low intracellular solubility, which exert pressure on the interior side of erythrocyte membrane causing mechanical distortion of the erythrocytes (sickle shape) (Rotter et al. 2005). Sodium metabisulfite ($\text{Na}_2\text{S}_2\text{O}_5$) is often used to induce poly-dHbS-M in vitro, which by virtue of its reducing property triggers low oxygen tension required for aggregation of dHbS-M, engendering morphologically distorted erythrocytes (Oyewole et al. 2008; Uwakwe and Nwaoguikpe, 2008; Nurain et al. 2017).

Epidemiological surveys showed that sickle cell disease (SCD) exerts an enormous burden on public health care system (Stallworth et al. 2010; Adewoyin et al. 2015). Estimates show that SCD affects 20–25 million people globally (Mulumba and Wilson, 2015) and approximately 300,000 children with SCD are born every year in the world, of which 75% of these births are in Sub-Saharan Africa (Diallo and Tcherna 2002; Weatherall et al. 2006; World Health Organization Regional Office for Africa, 2010; Makani et al. 2013). The dilapidating health challenges and disability-adjusted lifestyle of SCD sufferers are mostly impacted in developing countries (Weatherall et al. 2006). In Africa, SCD accounts for 50–90% rate of childhood mortality (Grosse et al. 2011). Global epidemiological surveys

and the prevalence of SCD is exhaustively reported elsewhere (Mulumba and Wilson 2015). The pathophysiology of SCD is such that management of the disease is often restricted to the use of prophylaxis in concert with drugs that ameliorate the disease symptoms, which offer no therapeutic benefits in form of radical cure.

Presently, hydroxyurea and 2-imidazolines are notable few clinical useful anti-sickling agents that reduce the frequency and severity of sickle cell crises (Chang et al. 1983; Charache et al. 1995; Stallworth et al. 2010; Makani et al. 2013). Hydroxyurea and 5-azacytidine induce the expression of fetal hemoglobin (HbF) via epigenetic regulation of globin gene expression in adult life (Frenette and Atweh 2007). HbF interferes and disrupts aggregation of dHbS-M in sickle cell anemia patients by virtue of its γ^{87} glutamine (Gln-gamma87) that impedes critical lateral contact regions on the double strand of HbS polymer (Charache et al. 1995; Setty et al. 2000; Cokic et al. 2003; Frenette and Atweh 2007; Eaton and Bunn 2017; Kassa et al. 2019). Toxicity associated with the use of hydroxyurea and 5-azacytidine has previously been reported (Eliot et al. 2006; Frenette and Atweh 2007; Oyewole et al. 2008; Kapoor et al. 2018).

Therapeutic approaches to radical cure of SCD, namely bone marrow transplantation, stem cell transplantation, and gene replacement therapy, in developing countries such as Nigeria and elsewhere, are expensive and remain inaccessible to the vast majority of SCD sufferers (Makani et al. 2013). Where the technology and expertise are available, there are still barriers to the suitability of donors, possibility of immunologic transplant rejection, prognostic uncertainty coupled with end-organ dysfunction, as well as long-term adverse outcomes, which is especially problematic for older patients (Frenette and Atweh 2007; Makani et al. 2013; Kapoor et al. 2018).

The use of prenatal prognostic evaluations, such as amniocentesis, as preventive measures against SCD, is not readily available in Sub-Saharan Africa for the fact the application of this technology is often scarce and expensive where available. Regrettably, clinical counseling to prospective biological parents of SCD sufferers, based on amniocentesis outcome, may advise termination of pregnancy before term, which is often untenable because of negative ethical and cultural considerations.

Chromatographic/spectrometric systems such as gas chromatography-mass spectrometry (GC-MS), Fourier transform-infrared spectrometry (FT-IR), and ultraviolet-visible spectroscopy (UV-visible) are used for chemical screening or metabolite profiling of herbal extracts (Sasidharan et al. 2011; Rašković et al. 2015; Chikezie et al. 2015; Ighodaro et al. 2016; Hemavathy et al. 2019). Molecular probe on establishing the structural identities of unknown organic molecules in complex mixtures and the

vast array of phytochemicals in herbal extracts is achieved by matching the spectra being investigated with reference and standard mass spectra from the library database {National Institute of Standards and Technology (NIST08) library and Wiley7n.1 libraries} (Semwa and Painuli 2019). Furthermore, FT-IR and UV-visible protocols are applied in elucidating structural conformations and molecular nature of functional groups of phytochemicals (Karayil et al. 2014; Rašković et al. 2015; Chikezie et al. 2015).

Previous studies, based on *in vitro* studies, revealed that the use of vast varieties of crude herbal extracts provides an approach to impede poly-dHbS-M (Oyewole et al. 2008; Chikezie, 2011; Dash et al. 2013; Nurain et al. 2017). Because of physicochemical diversity of vast combinations of phytochemicals from crude herbal extracts, we hypothesize that fractionated leaf extracts of cashew (*Anacardium occidentale* Linn.), guava (*Psidium guajava* Linn.), and Indian almond (*Terminalia catappa* Linn.) will exhibit differential capacities to alter the process leading to the poly-dHbS-M. The present study evaluated levels of poly-dHbS-M in the presence of fractionated leaf extracts of *A. occidentale*, *P. guajava*, and *T. catappa* using *in vitro* models. Furthermore, the phytochemicals from fractionated leaf extracts of *A. occidentale*, *P. guajava*, and *T. catappa* that exhibited comparatively high potency to impede poly-dHbS-M, or otherwise, were identified, quantified, and characterized using combined GC-MS, FT-IR and UV-visible systems protocols.

Methods

Collection and preparation of leaf samples

Fresh leaves of *A. occidentale*, *P. guajava*, and *T. catappa* were harvested during the wet season (3rd–7th April 2019) from private botanical gardens within the environment of Imo State University, Owerri (Latitude 5° 30.2237' N; Longitude 7° 2.6277' E), which lies on the rainforest belt of Nigeria. The seeds of the plants were obtained in the wild as non-commercial materials and permissions were not necessary to collect such samples. The collection of plant materials complied with institutional, national, and international guidelines as well as in accordance with local legislation. The harvested leaves of the selected plants used in the present study were identified and authenticated by Professor F.N. Mbagwu of the Department of Plant Science and Biotechnology, Imo State University, Owerri, Nigeria. The voucher numbers were assigned as follows: *A. occidentale*: IMSUH-009; *P. guajava*: IMSUH-010; *T. catappa*: IMSUH-011 and the plant specimens were deposited in the department herbarium.

Thereafter, the leaves were washed and air-dried at ambient laboratory temperature of 25 ± 5 °C pending extraction within 24 h of collection of the leaf samples.

The preparation of the leaves for extraction was according to the methods previously described (Ojiako et al. 2015). Eight hundred grams (800 g) part of the chopped fresh leaves were weighed using a triple beam balance (OHAU 750-50; OHAUS Triple Beam Balance, Model TJ611, Burlington, NC, USA) and dried to constant weight in an oven (WTC BINDER; 7200 Tuttlinge, Germany) at 50 °C for 10–12 h as previously described (Ezekwe and Chikezie 2017). Thomas-Willey milling machine (ASTM D-3182; India) was used to grind the dried leaf samples into powder. The powdered leaf samples were sieved on a wire mesh screen (1 × 1 mm²) to remove relatively large particles. Finally, the fine ground leaf samples were stored at 4 °C in air-tight screw-capped bottles pending extraction and fractionation.

Extraction and fractionation of leaf extracts

Extraction of 300 g of the dried ground samples was carried out in 2000 mL of ethanol/water mixture; 1:1 v/v using repeated cycles of Soxhlet extraction protocol for 18 h to obtain a final volume of 500 mL of each herbal extracts (Ojiako et al. 2015). Preparation of fractionated leaf extracts of *A. occidentale*, *P. guajava*, and *T. catappa* was according to the methods previously described by Okoye et al. (2010) but with modifications. Separate volumes of the crude hydro-ethanolic leaf extracts were transferred into corresponding separating funnels. Fractionation of the crude hydro-ethanolic leaf extracts was carried out by successive partitioning using equal volumes of solvents in the order of increasing polarities, namely petroleum ether, *n*-hexane, chloroform, and ethylacetate.

Corresponding fractionated leaf extracts, namely petroleum ether-, *n*-hexane-, chloroform-, ethylacetate-, as well as the residual aqueous extracts, were concentrated under reduced pressure in a rotary evaporator (Büch Rotavapor R-200) for 12 h at 50 °C and the residues dried in a vacuum desiccator. The yield of the fractionated leaf extracts was calculated as ratio of dried weight of the extract to 100 g of the dried ground leaf sample. Portions of the fractionated leaf extracts were suspended in measured volumes of phosphate-buffered saline (PBS); pH = 7.4, osmotically equivalent to 9.0 g/L sodium chloride (NaCl) {9.0 g NaCl, 1.71 g Na₂HPO₄·2H₂O, and 2.43 g NaH₂PO₄·2H₂O per liter} to give standard solutions of the extracts used for HbS polymerization studies.

Exclusion criteria

The guidelines previously reported (Yamamoto et al. 2014) was used as bases for exclusion criteria for participants. The exclusion criteria include participants who were on routine medications, received blood transfusion and infusion for at least 4 weeks prior to blood sampling. Furthermore, blood samples were thoroughly

cross-checked for the presence of clot before used for the experiment.

Collection and preparation of blood samples

Venous blood samples were collected by venipuncture, between 7th of May and 28th of July, 2019, from 108 consenting individuals of homozygous sickle hemoglobin (HbSS) genotype under the auspices of Rehoboth Christian Medical Center, Nwaoruebi and Easter Summit Specialist Clinics and Maternity, Amakohia. The clinics are located in Imo State, Owerri, Nigeria. The blood samples were stored in EDTA anticoagulant tubes. The genotype of the blood samples was further subjected to a confirmatory test using cellulose acetate electrophoretic methods previously described (Bain et al. 2012).

The HbS erythrocytes were washed using centrifugation methods as described (Tsakiris et al. 2005) with modifications according to previous reports (Chikezie, 2011; Chikezie and Uwakwe 2011). Within 2 h of collection of the blood sample, a portion of 4.0 mL of the sample was introduced into a centrifuge test tube containing 4.0 mL of PBS; pH = 7.4. The erythrocytes were separated from plasma by centrifugation at 1200xg for 10 min. The protocol was repeated three times. The erythrocytes were finally re-suspended in 5.0 mL of PBS and used for polymerization studies of dHbS-M.

Sickle hemoglobin polymerization studies

Polymerization studies of dHbS-M were carried out according to the modified methods previously described (Chikezie 2011), whereby non-hemolyzed HbSS erythrocytes were used instead of hemolysate samples. A 0.1 mL of HbSS erythrocyte suspension (10% hematocrit) was mixed with 0.5 mL PBS, followed by the introduction of an additional 1.0 mL of PBS in a test tube. The mixture was transferred into a cuvette and 3.4 mL of 2.0 g/100 mL aqueous solution of Na₂S₂O₅ was added. The absorbance of the assay mixture was measured at a maximum wavelength (λ_{max}) = 700 nm, at regular intervals of 30 s for 180 s, using a spectrophotometer (Digital Blood Analyzer; SPECTRONIC 20; Labtech, LabX, Bay Street, Midland, ON, Canada) (control assay). The procedure was repeated substituting the 1.0 mL of PBS with corresponding three increasing concentrations (40, 60, and 80 mg/100 mL) of each of the separate fractionated leaf extracts (test assay). Relative poly-dHbS-M (%) was calculated according to the formula previously described (Chikezie et al. 2010; Chikezie 2011).

$$\%RP = \frac{A_{t/c}}{A_{c\ 180^{th}\ s}} \times 100 \tag{1}$$

where:

%RP: relative poly-dHbS-M (%)

A_{t/c}: absorbance of test/control sample at a given time (second)

A_{c180th s}: absorbance of control sample at the 180th second

Inhibition/activation of poly-dHbS-M

Arithmetically, the percentage inhibition/activation of poly-dHbS-M by the leaf extracts at a given experimental time interval was obtained thus:

$$\%I\A = \%PC_{ct} - \%PT_{ct} \tag{2}$$

where:

%I\A: percentage inhibition or activation of poly-dHbS-M

%PC_{ct}: %RP of the control sample at a given experimental time interval

%PT_{ct}: %RP of the test sample at a given experimental time interval corresponding to that of the control sample

Note: The algebraic sum of percentage activation of poly-dHbS-M is negative, whereas percentage inhibition of poly-dHbS-M is positive in the presence of the leaf extract.

Cumulative polymerization index

The cumulative inhibition/activation of poly-dHbS-M within the experimental time of 180 s is defined by a measure of the Area under the Curve (AUC) of the plot of %RP versus time (s).

Using the Simpson’s rule, thus:

$$f(x_1)h_1 + f(x_2)h_2 + \dots + f(x_n)h_n$$

This is given by:

$$\begin{aligned} \text{AUC (polymerization}\%.\text{second)} \\ = \frac{t}{2} (x_n + 2x_{n-1} + 2x_{n-2} + 2x_{n-3} + \dots x_{n-\infty}) \end{aligned} \tag{3}$$

where:

t: time intervals of 30 s

x: %RP at corresponding time interval

Thus:

$$\text{RCPI}\% = \frac{\text{AUC}_{\text{Control}} - \text{AUC}_{\text{Test}}}{\text{AUC}_{\text{Control}}} \times 100 \tag{4}$$

where:

RCPI%: relative cumulative polymerization index

Note: A positive RCPI% connotes cumulative inhibition of poly-dHbS-M, whereas negative RCPI% connotes cumulative activation of poly-dHbS-M by the leaf extract.

Spectrometry

The identification, quantification, and characterization of phytochemicals from fractionated leaf extracts of *A. occidentale*, *P. guajava*, and *T. catappa* were carried out using standard chromatographic/spectrometric protocols, viz. GC-MS systems (Agilent 7890A GC system set up with 5975C VL MSD, Agilent Technologies, Inc., Santa Clara, CA, USA) operated as previously described (Rašković et al. 2015). The MS system was accomplished in electron ionization (EI) mode with selected ion monitoring (SIM). FT-IR and UV-visible instruments (PerkinElmer Spectrophotometer, USA) were performed according to the methods previously described (Ighodaro et al. 2016; Hemavathy et al. 2019).

Statistical analyses

The data collected were expressed in means (\bar{X}) \pm SD and analyzed in one-way ANOVA and least significance difference (LSD). The comparison was made between groups and significance was established by ANOVA at 95% confidence level. The difference of $p < 0.05$ was considered statistically significant.

Results

Percentage yields of fractionated leaf extracts

The percentage yields of the fractionated leaf extracts of *A. occidentale*, *P. guajava*, and *T. catappa* are presented in Table 1. The aggregate yields of petroleum ether, *n*-hexane, chloroform, ethylacetate, and residual aqueous fractions of the leaf extracts were *A. occidentale* (13.017 g per 100 g dry leaf sample), *P. guajava* (9.627 g per 100 g dry leaf sample), and *T. catappa* (10.060 g per 100 g dry leaf sample). The residual aqueous fractions of the leaf extracts gave corresponding highest percentage yields (Table 1).

Levels of poly-dHbS-M in the presence of fractionated leaf extracts of *A. occidentale*

Figure 1a–e showed the levels of poly-dHbS-M of the control sample and in the presence of fractionated leaf extract of *A. occidentale* with the progression of experimental time. The control sample exhibited a comparatively higher level of poly-dHbS-M than those of the samples containing 40, 60, and 80 mg/100 mL petroleum ether extracts of *A. occidentale* within the experimental time range of $0 \text{ s} \leq t \leq 120 \text{ s}$ (Fig. 1a).

Specifically, at $t = 30 \text{ s}$, 40 mg/100 mL petroleum ether extract of *A. occidentale* caused significantly lower ($p < 0.05$) level of poly-dHbS-M than the control sample as well as the samples containing 60 and 80 mg/100 mL petroleum ether extracts of *A. occidentale* (Fig. 1a). Conversely, at $t = 30 \text{ s}$, the levels of poly-dHbS-M of the control sample, as well as the samples containing 60 and 80 mg/100 mL petroleum ether extracts of *A. occidentale*, showed no significant difference ($p > 0.05$).

Figure 1b showed the levels of poly-dHbS-M of the control sample and samples containing *n*-hexane extract of *A. occidentale*. An overview of Fig. 1b showed that the pattern of levels of poly-dHbS-M of the control sample and sample containing 80 mg/100 mL *n*-hexane extract of *A. occidentale* were biphasic. For instance, at $t < 60 \text{ s}$, the control sample and sample containing 80 mg/100 mL *n*-hexane extract of *A. occidentale* exhibited exponential increasing levels of poly-dHbS-M, which was followed by a phase of decreasing levels of poly-dHbS-M. The peak levels of poly-dHbS-M of samples containing 40 and 60 mg/100 mL *n*-hexane extracts of *A. occidentale* occurred at $t = 90 \text{ s}$, which was followed by moderate decreasing levels of poly-dHbS-M as experimental time progressed. The maximum level of poly-dHbS-M of the control sample, at $t = 60 \text{ s}$, was significantly higher ($p < 0.05$) than those of samples containing 40, 60, and 80 mg/100 mL *n*-hexane extracts of *A. occidentale*. Conversely, at $t = 180 \text{ s}$, the levels of poly-dHbS-M of the sample containing 40, 60, and 80 mg/100 mL *n*-hexane extracts of *A. occidentale* were significantly higher ($p < 0.05$) than that of the control sample.

Figure 1c showed that the pattern of levels of poly-dHbS-M of the control sample, as well as samples containing 40, 60, and 80 mg/100 mL chloroform extracts of *A. occidentale*, were biphasic. A peak level of poly-dHbS-M of the control sample was at $t = 90 \text{ s}$, whereas those of the samples containing 60 and 80 mg/100 mL chloroform extracts of *A. occidentale* were at $t = 60 \text{ s}$. Figure 1c showed that the level of poly-dHbS-M of the sample containing 40 mg/100 mL chloroform extract of *A. occidentale* peaked at $t = 30 \text{ s}$. An overview of Fig. 1c showed that 40 and 60 mg/100 mL chloroform extracts of *A. occidentale* caused significant higher ($p < 0.05$) levels of poly-dHbS-M compared with that of the control sample. Additionally, within the experimental time

Table 1 Yields of fractionated leaf extracts

Extract fractions	Yield (g per 100 g dry leaf sample); w/w ratio				
	Petroleum ether	<i>n</i> -hexane	Chloroform	Ethylacetate	Residual aqueous
<i>A. occidentale</i>	2.017	0.470	0.177	0.153	10.20
<i>P. guajava</i>	1.091	0.763	0.100	0.473	7.20
<i>T. catappa</i>	0.340	0.630	0.013	0.077	9.00

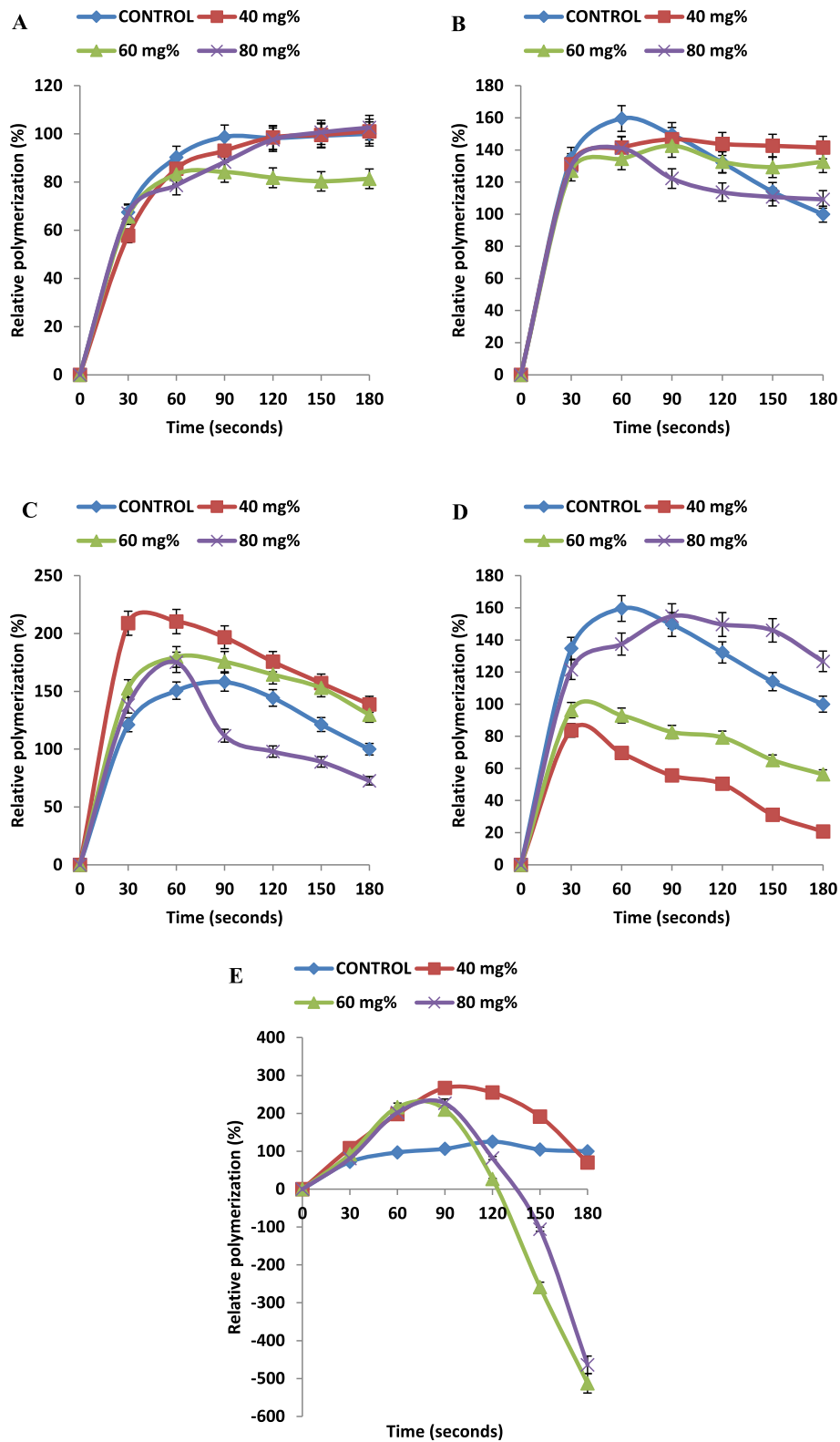


Fig. 1 Comparative levels of poly-dHbS-M of control sample and in the presence of fractionated leaf extracts of *A. occidentale*. **a** Petroleum ether. **b** *n*-hexane. **c** Chloroform. **d** Ethylacetate. **e** Residual aqueous; mg% = mg/100 mL

of $t < 60$ s, the sample containing 80 mg/100 mL chloroform extract exhibited a significant higher ($p < 0.05$) level of poly-dHbS-M. Conversely, at $t > 60$ s, 80 mg/100 mL chloroform extract caused significantly lower ($p < 0.05$) level of poly-dHbS-M compared with the control sample.

Figure 1d showed the biphasic pattern of levels of poly-dHbS-M of the control sample as well as that of the samples containing 40, 60, and 80 mg/100 mL ethylacetate extracts of *A. occidentale*, in which the samples exhibited an exponential increase in their levels of poly-dHbS-M within the experimental time of $t < 30$ s.

Figure 1d showed that the control sample gave a peak level of poly-dHbS-M at $t = 60$ s, whereas that of 80 mg/100 mL ethylacetate extract of *A. occidentale* peaked at $t = 90$ s. Additionally, the peak levels of poly-dHbS-M of the samples containing 40 and 60 mg/100 mL ethylacetate extracts of *A. occidentale* occurred at $t = 30$ s. The level of poly-dHbS-M of the control sample was significantly higher ($p < 0.05$) than those of the samples containing 40, 60, and 80 mg/100 mL ethylacetate extracts of *A. occidentale* at $t < 60$ s (Fig. 1d). Conversely, at $t > 90$ s, the sample containing 80 mg/100 mL ethylacetate extract of *A. occidentale* exhibited significantly higher ($p < 0.05$) levels of poly-dHbS-M than the control sample and samples containing 40 and 60 mg/100 mL ethylacetate extracts of *A. occidentale*. The sample containing 40 mg/100 mL ethylacetate extract of *A. occidentale* gave the lowest level of poly-dHbS-M compared with other experimental samples ($p < 0.05$).

Figure 1e showed that the maximum level of poly-dHbS-M of the control sample was at $t = 120$ s, whereas those of the sample containing 40, 60, and 80 mg/100 mL residual aqueous extracts of *A. occidentale* peaked at $t = 90$ s. Furthermore, the levels of poly-dHbS-M of the sample containing 40, 60, and 80 mg/100 mL residual aqueous extracts of *A. occidentale* were significantly higher ($p < 0.05$) than that of the control sample. However, at $t > 120$ s, the sample containing 60 and 80 mg/100 mL residual aqueous extracts of *A. occidentale* exhibited exponential decreasing levels of poly-dHbS-M, which were significantly lower ($p < 0.05$) than that of the control sample. The levels of poly-dHbS-M of samples containing 60 and 80 mg/100 mL residual aqueous extracts of *A. occidentale* gave negative numerical values at approximately $t > 120$ s and $t > 135$ s respectively (Fig. 1e). At the end of the experimental time, the levels of poly-dHbS-M of the sample containing 40, 60, and 80 mg/100 mL residual aqueous extracts of *A. occidentale* were significantly lower ($p < 0.05$) than that of the control sample. Within the experimental time range of $90 \text{ s} \leq t \leq 150 \text{ s}$, the level of poly-dHbS-M of the sample containing 40 mg/100 mL residual aqueous extract of *A. occidentale* was significantly higher ($p < 0.05$) than that of the control sample.

Levels of poly-dHbS-M in the presence of fractionated leaf extracts of *P. guajava*

The levels of poly-dHbS-M of the control sample and in the presence of fractionated leaf extracts of *P. guajava* with experimental time are presented in Fig. 2a–e. Figure 2a showed that the levels of poly-dHbS-M of the control sample and the samples containing 40, 60, and 80 mg/100 mL petroleum ether extracts of *P. guajava* were biphasic. The first phase showed an exponentially increasing level of poly-dHbS-M of the control sample, which peaked at $t = 90$ s. The levels of poly-dHbS-M of the test samples peaked at $t = 60$ s. It is worthwhile to note that the levels of poly-dHbS-M of the samples containing 40, 60, and 80 mg/100 mL petroleum ether extracts of *P. guajava* showed no significant difference ($p > 0.05$) within the experimental time of $t < 90$ s.

Figure 2a showed that the second phase of poly-dHbS-M of the control sample and the sample containing 40, 60, and 80 mg/100 mL petroleum ether extracts of *P. guajava* exhibited decreasing levels of poly-dHbS-M as experimental time increased. Additionally, the decreasing levels of poly-dHbS-M of the test samples were depended on the concentrations of the herbal extracts, which were in the order: 80 mg/100 mL > 60 mg/100 mL > 40 mg/100 mL. Overall, the level of poly-dHbS-M of the control sample was significantly lower ($p < 0.05$) than those of the test samples.

Figure 2b showed the levels of poly-dHbS-M of the control and test samples. The pattern of level of poly-dHbS-M of the sample containing 80 mg/100 mL *n*-hexane extract of *P. guajava* was biphasic. The levels of poly-dHbS-M of the samples containing 40, 60, and 80 mg/100 mL *n*-hexane extracts of *P. guajava* were significantly different ($p < 0.05$) within the experimental time; except at $t = 90$ s.

Figure 2c showed that, within the experimental time range of $90 \text{ s} \leq t \leq 180 \text{ s}$, the level of poly-dHbS-M of the control sample was significantly higher ($p < 0.05$) than those of the samples containing 40, 60, and 80 mg/100 mL chloroform extracts of *P. guajava*. Conversely, the levels of poly-dHbS-M of the control and test samples exhibited no significant difference ($p > 0.05$) within the experimental time of $t < 90$ s. The pattern of levels of poly-dHbS-M of the test samples was biphasic, which exhibited an exponential increase in the level of poly-dHbS-M at $t < 60$ s; $p > 0.05$.

Figure 2d showed that the levels of poly-dHbS-M of the samples containing 40 and 80 mg/100 mL ethylacetate extracts of *P. guajava* were significantly lower ($p < 0.05$) than that of the control sample. Conversely, the level of poly-dHbS-M of the sample containing 60 mg/100 mL ethylacetate extract of *P. guajava* was significantly higher ($p < 0.05$) than that of the control sample. An overview of Fig. 2d showed that the pattern of levels of poly-dHbS-M

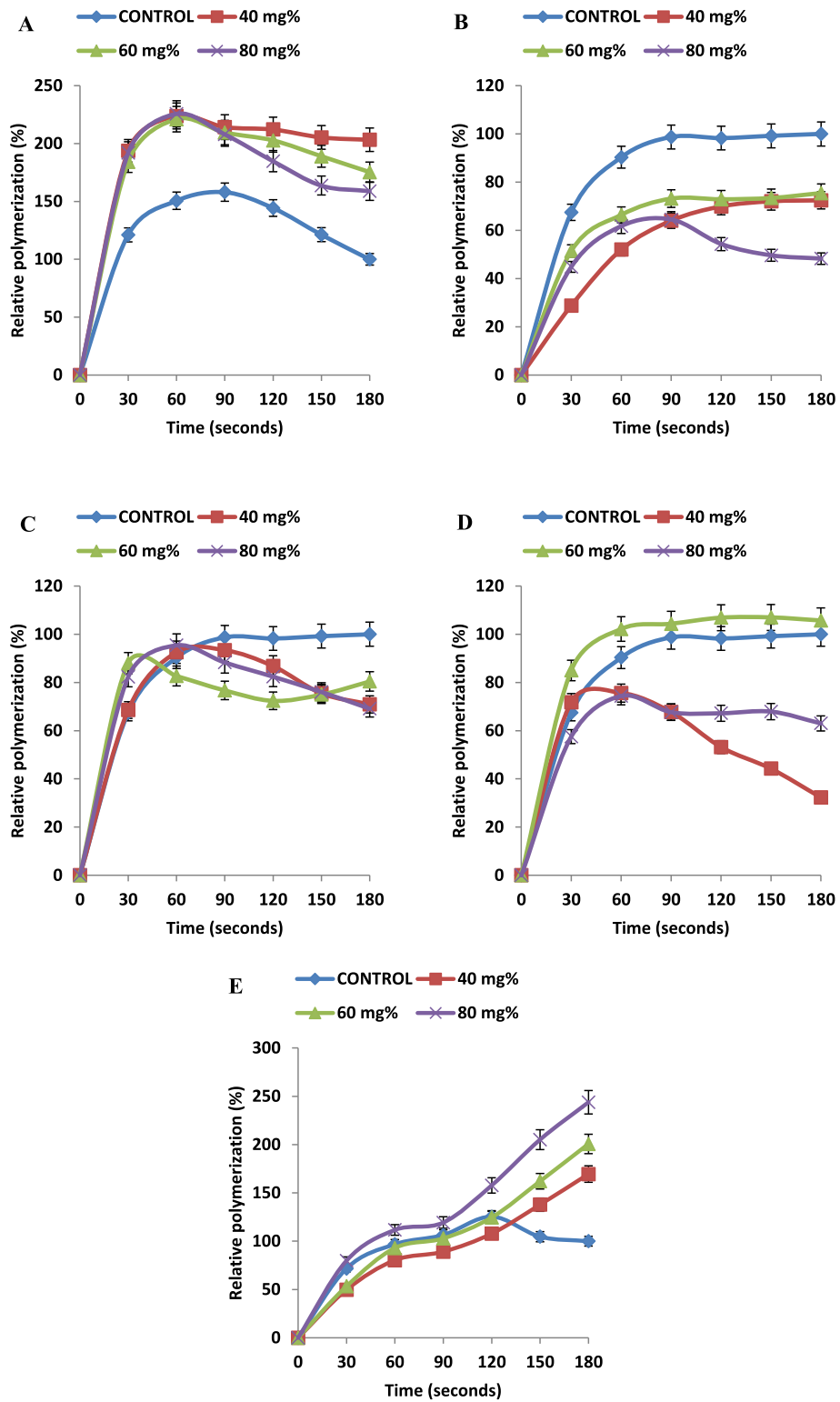


Fig. 2 Comparative levels of poly-dHbS-M of control sample and in the presence of fractionated leaf extracts of *P. guajava*. **a** Petroleum ether. **b** *n*-hexane. **c** Chloroform. **d** Ethylacetate. **e** Residual aqueous; mg% = mg/100 mL

of 40 and 80 mg/100 mL ethylacetate extracts of *P. guajava* was biphasic. Additionally, the levels of poly-dHbS-M in the presence of 40 and 80 mg/100 mL ethylacetate extracts of *P. guajava* showed no significant difference ($p > 0.05$) within the time range of $60 \text{ s} \leq t \leq 90 \text{ s}$, in which the peak value of poly-dHbS-M was at $t = 60 \text{ s}$. The levels of poly-dHbS-M of the control sample and the sample containing 40 mg/100 mL ethylacetate extract of *P. guajava* showed no significant difference at $t < 30 \text{ s}$ ($p > 0.05$).

Figure 2e showed that within the experimental time range of $90 \text{ s} \leq t \leq 180 \text{ s}$, the increasing levels of poly-dHbS-M of the test samples were in a concentration-dependent manner; i.e., 80 mg/100 mL > 60 mg/100 mL > 40 mg/100 mL. However, the level of poly-dHbS-M of 40 mg/100 mL residual aqueous extract of *P. guajava* was significantly lower ($p < 0.05$) than that of the control sample at $t < 120 \text{ s}$. Likewise, the level of poly-dHbS-M of the sample containing 60 mg/100 mL of residual aqueous extract was significantly lower ($p < 0.05$) than that of the control sample at $t = 30 \text{ s}$, which was contrary within the time range of $60 \text{ s} \leq t \leq 120 \text{ s}$; $p > 0.05$ (Fig. 2e).

Within the experimental time, the level of poly-dHbS-M of the sample containing 80 mg/100 mL residue aqueous extract of *P. guajava* was significantly higher ($p < 0.05$) than that of the control sample. Furthermore, at $t > 120 \text{ s}$, the levels of poly-dHbS-M of the sample containing 40, 60, and 80 mg/100 mL residue aqueous extracts of *P. guajava* were significantly higher ($p < 0.05$) than that of the control sample. The level of poly-dHbS-M of the control sample was biphasic with a peak value at $t = 120 \text{ s}$ (Fig. 2e).

Levels of poly-dHbS-M in the presence of fractionated leaf extracts of *T. catappa*

Figure 3a–e showed the levels of poly-dHbS-M of the control sample and the samples containing 40, 60, and 80 mg/100 mL of fractionated leaf extracts of *T. catappa* with experimental time. Figure 3a showed that the pattern of levels of poly-dHbS-M of the test samples was biphasic. The levels of poly-dHbS-M of the samples containing 40, 60, and 80 mg/100 mL petroleum ether extracts peaked at $t = 90 \text{ s}$, $t = 90 \text{ s}$, and $t = 30 \text{ s}$ respectively. The levels of poly-dHbS-M of the samples containing 60 and 80 mg/100 mL of petroleum ether extracts were significantly lower ($p < 0.05$) than that of the control sample at $t > 150 \text{ s}$, whereas the sample containing 40 mg/100 mL petroleum ether extract showed no significant difference ($p > 0.05$) from that of the control sample at $t = 180 \text{ s}$.

Figure 3b showed that within the experimental time of $t < 90 \text{ s}$, the levels of poly-dHbS-M of the samples containing 40, 60, and 80 mg/100 mL *n*-hexane extracts of *T. catappa* were significantly higher ($p < 0.05$) than the control sample. Conversely, at $t > 120 \text{ s}$, the levels of

poly-dHbS-M of the test samples was significantly lower ($p < 0.05$) than that of the control sample.

Within the experimental time of $t < 180 \text{ s}$, the level of poly-dHbS-M of the sample containing 80 mg/100 mL chloroform extract of *T. catappa* was significantly lower ($p < 0.05$) than that of the control sample (Fig. 3c). Likewise, the sample containing 60 mg/100 mL chloroform extract of *T. catappa* gave significantly lower ($p < 0.05$) level of poly-dHbS-M within the experimental time range of $60 \text{ s} \leq t \leq 120 \text{ s}$. The levels of poly-dHbS-M of the samples containing 40 and 60 mg/100 mL chloroform extracts of *T. catappa* were significantly higher ($p < 0.05$) than that of the control sample at $t = 30 \text{ s}$. Additionally, at $t > 150 \text{ s}$, the level poly-dHbS-M of the sample containing 40 mg/100 mL chloroform extract was significantly higher ($p < 0.05$) than that of the control sample.

Figure 3d showed that within the experimental time, $t > 120 \text{ s}$, the level of poly-dHbS-M of the sample containing 40 mg/100 mL ethylacetate extract of *T. catappa* was significantly higher ($p < 0.05$) than that of the control sample. The levels of poly-dHbS-M of test samples showed no significant difference ($p > 0.05$) from that of the control sample at $t = 30 \text{ s}$. Furthermore, at $t = 60 \text{ s}$, the level of poly-dHbS-M in the presence of the sample containing 40 mg/100 mL ethylacetate extract of *T. catappa* was significantly lower ($p < 0.05$) than that of the control sample. Within the experimental time, the levels of poly-dHbS-M of the test samples were significantly different ($p < 0.05$) in a concentration-dependent manner; except between samples containing 40 and 60 mg/100 mL ethylacetate extract of *T. catappa* at $t = 60 \text{ s}$; $p > 0.05$.

Figure 3 showed that within the experimental time, the level of poly-dHbS-M of the sample containing 40 mg/100 mL residual aqueous extract of *T. catappa* was significantly higher ($p < 0.05$) than those of the control sample as well as the samples containing 60 and 80 mg/100 mL residual aqueous extracts of *T. catappa*; except at $t = 180 \text{ s}$; $p > 0.05$.

The level of poly-dHbS-M of the sample containing 60 mg/100 mL residue aqueous extract of *T. catappa* was significantly lower ($p < 0.05$) than that of the control sample at $t < 120 \text{ s}$. The level of poly-dHbS-M of the sample containing 80 mg/100 mL residual aqueous extract of *T. catappa* was significantly lower ($p < 0.05$) than that of the control sample at $t < 120 \text{ s}$; but was not significantly different ($p > 0.05$) from that of the control sample at $t = 30 \text{ s}$. At the end of the experimental time, the level of poly-dHbS-M of the test samples was significantly higher ($p < 0.05$) than that of the control sample (Fig. 3e).

Percentage inhibition/activation of poly-dHbS-M in the presence of fractionated leaf extracts

Table 2 showed the percentage inhibition/activation of poly-dHbS-M in the presence of varying concentrations

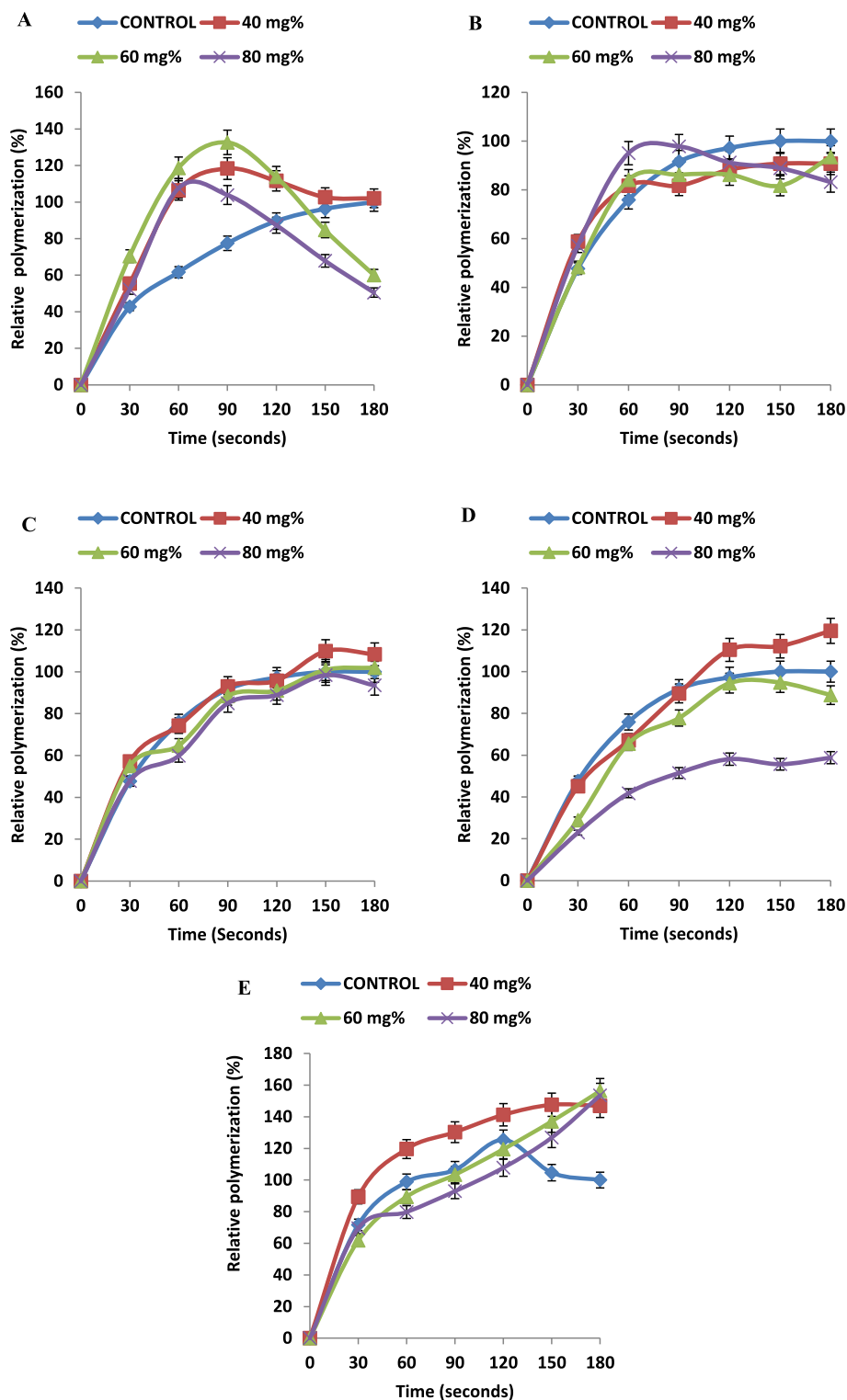


Fig. 3 Comparative levels of poly-dHbS-M of control sample and in the presence of fractionated leaf extracts of *T. catappa*. **a** Petroleum ether. **b** *n*-hexane. **c** Chloroform. **d** Ethylacetate. **e** Residual aqueous; mg% = mg/100 mL

Table 2 Relative levels of inhibition/activation of poly-dHbS-M by fractionated leaf extracts of *A. occidentale*, *P. guajava*, and *T. catappa*

[Extract fraction]	Relative inhibition/activation of polymerization (%)					
	30 s	60 s	90 s	120 s	150 s	180 s
<i>A. occidentale</i> petroleum ether						
40 mg%	9.76 ± 1.23	4.83 ± 0.73	5.76 ± 1.10	0.25 ± 0.05↑	0.31 ± 0.02↑	1.06 ± 0.02↑
60 mg%	1.74 ± 0.02	7.10 ± 1.11	14.57 ± 1.12	16.49 ± 1.22	18.39 ± 1.11	18.65 ± 1.10
80 mg%	0.38 ± 0.01	11.68 ± 0.89	10.43 ± 1.08	0.66 ± 0.01	1.43 ± 0.02↑	2.60 ± 0.88↑
<i>A. occidentale</i> n-hexane						
40 mg%	3.70 ± 0.04	18.15 ± 1.21	2.96 ± 0.03	11.48 ± 1.10↑	28.52 ± 2.80↑	41.48 ± 3.87↑
60 mg%	7.77 ± 1.56	25.19 ± 2.56	7.04 ± 1.16	0.37 ± 0.01↑	15.19 ± 1.80↑	32.59 ± 3.67↑
80 mg%	4.81 ± 1.65	18.52 ± 2.01	27.41 ± 2.98	18.51 ± 2.07	3.33 ± 0.98	9.26 ± 1.67↑
<i>A. occidentale</i> chloroform						
40 mg%	87.80 ± 4.90↑	59.83 ± 5.91↑	38.69 ± 2.10↑	31.25 ± 2.20↑	35.84±3.00↑	38.69 ± 4.01↑
60 mg%	31.25 ± 3.67↑	29.17 ± 3.23↑	17.55 ± 1.10↑	20.24 ± 1.90↑	31.67 ± 3.00↑	29.76 ± 2.67↑
80 mg%	16.97 ± 2.88↑	24.41 ± 3.11↑	46.43 ± 3.56	46.42 ± 2.56	32.31 ± 2.54	27.38 ± 2.56
<i>A. occidentale</i> ethylacetate						
40 mg%	51.11 ± 4.98	90.00 ± 5.78	94.07 ± 6.98	81.85 ± 5.34	82.96 ± 4.87	79.26 ± 4.98
60 mg%	38.51 ± 2.80	66.67±3.48	67.04 ± ± 3.95	52.96 ± 3.01	48.88 ± 3.89	43.71 ± 2.69
80 mg%	13.33 ± 1.80	22.22 ± 2.00	5.18 ± 1.01↑	17.41 ± 1.90↑	31.85 ± 2.50↑	26.67 ± 2.11↑
<i>A. occidentale</i> residual aqueous						
40 mg%	36.64 ± 3.00↑	101.13 ± 7.9↑	160.61 ± 8.9↑	129.53 ± 7.1↑	87.03 ± 4.10↑	29.93 ± 2.78
60 mg%	20.59 ± 2.00↑	119.63 ± 9.7↑	103.75 ± 7.9↑	98.44 ± 5.40↑	363.18 ± 11.8	612.46 ± 15.9
80 mg%	9.28 ± 1.76↑	105.26 ± 8.6↑	120.11 ± 8.9↑	43.34 ± 2.52	210.72 ± 10.7	563.95 ± 13.8
<i>P. guajava</i> petroleum ether						
40 mg%	72.62 ± 3.50↑	73.22 ± 2.89↑	56.25 ± 4.97↑	67.86 ± 3.55↑	84.06 ± 4.01↑	103.27 ± 7.4↑
60 mg%	63.10 ± 4.10↑	70.54 ± 4.92↑	51.48 ± 3.87↑	58.34 ± 2.98↑	67.69 ± 4.91↑	75.30 ± 3.77↑
80 mg%	70.83 ± 3.80↑	75.16 ± 3.78↑	49.99 ± 2.99↑	40.48 ± 3.32↑	42.39 ± 4.11↑	58.93 ± 4.54↑
<i>P. guajava</i> n-hexane						
40 mg%	38.68 ± 2.98	38.31 ± 3.00	34.71 ± 2.09	28.33 ± 2.98	27.15 ± 2.67	27.54 ± 2.67
60 mg%	16.00 ± 1.76	23.90 ± 1.98	25.54 ± 1.77	25.39 ± 2.00	25.79 ± 2.08	34.53 ± 2.33
80 mg%	22.60 ± 2.76	28.56 ± 2.78	34.23 ± 3.03	43.94 ± 3.66	49.57 ± 3.89	51.73 ± 4.03
<i>P. guajava</i> chloroform						
40 mg%	1.10 ± 0.09↑	2.19 ± 0.86↑	5.37 ± 0.98	11.51 ± 1.09	23.72 ± 2.04	29.10 ± 2.54
60 mg%	20.56 ± 2.40↑	7.64 ± 0.99	22.00 ± 2.03	25.87 ± 1.78	24.23 ± 2/12	19.59 ± 2.03
80 mg%	14.81 ± 1.10↑	5.08 ± 0.89↑	10.42 ± 1.21	15.85 ± 1.78	23.13 ± 2.21	30.84 ± 2.78
<i>P. guajava</i> ethylacetate						
40 mg%	4.31 ± 0.09↑	14.75 ± 1.02	31.03 ± 2.45	45.10 ± 3.11	55.01 ± 3.08	67.73 ± 3.98
60 mg%	17.53 ± 1.60↑	11.84 ± 1.22↑	5.60 ± 0.98↑	8.59 ± 1.12↑	7.76 ± 1.11↑	5.68 ± 0.93↑
80 mg%	9.93 ± 1.02	15.93 ± 1.65	31.07 ± 2.34	31.06 ± 2.01	31.32 ± 2.33	37.00 ± 3.09
<i>P. guajava</i> residual aqueous						
40 mg%	22.01 ± 1.98	16.46 ± 1.56	17.29 ± 1.45	17.57 ± 1.87	33.18 ± 2.45↑	69.53 ± 5.34↑
60 mg%	18.38 ± 1.78	3.86 ± 1.32	3.54 ± 0.89	0.83 ± 0.08	57.40 ± 2.78↑	100.73 ± 8.8↑
80 mg%	8.08 ± 0.78↑	14.82 ± 1.78↑	12.84 ± 1.04↑	32.38 ± 2.02↑	100.53 ± 8.5↑	143.88 ± 9.8↑
<i>T. catappa</i> petroleum ether						
40 mg%	12.63 ± 1.40↑	44.78 ± 3.59↑	40.91 ± 4.0↑	22.06 ± 2.11↑	6.39 ± 1.23↑	2.02 ± 0.21↑

Table 2 Relative levels of inhibition/activation of poly-dHbS-M by fractionated leaf extracts of *A. occidentale*, *P. guajava*, and *T. catappa* (Continued)

[Extract fraction]	Relative inhibition/activation of polymerization (%)					
	30 s	60 s	90 s	120 s	150 s	180 s
60 mg%	27.61±2.20↑	57.07 ± ± 4.78↑	55.22 ± 5.2↑	24.25 ± 2.19↑	11.62 ± 1.05	39.90 ± 2.56
80 mg%	9.43 ± 0.56↑	45.96 ± 4.98↑	26.43 ± 3.1↑	2.18 ± 0.09	28.46 ± 1.45	49.50 ± 3.67
<i>T. catappa</i> <i>n</i> -hexane						
40 mg%	11.07 ± 1.9↑	5.81 ± 1.09↑	9.91 ± 1.08	8.88 ± 0.95	9.21 ± 0.17	9.21 ± 0.95
60 mg%	0.61 ± 0.03↑	8.23 ± 0.85↑	5.41 ± 0.09	11.00 ± 0.87	18.31 ± 2.01	6.50 ± 0.98
80 mg%	9.46 ± 0.97↑	19.16 ± 1.56↑	6.21 ± 1.54↑	5.99 ± 1.04	15.06 ± 1.67	16.81 ± 2.45
<i>T. catappa</i> chloroform						
40 mg%	9.46 ± 1.06↑	0.96 ± 0.02	1.35 ± 0.08↑	1.46 ± 0.09	9.87 ± 0.89↑	8.33 ± 1.02↑
60 mg%	7.29 ± 0.09↑	11.13±1.78	3.18 ± 0.45	1.46 ± 0.06	0.09 ± 0.001↑	1.89 ± 0.08↑
80 mg%	0.19 ± 0.09↑	16.02 ± 1.98	6.64 ± 1.07	8.32 ± 1.44	1.57 ± 0.07	6.44 ± 0.98
<i>T. catappa</i> ethylacetate						
40 mg%	2.53 ± 0.88	8.91 ± 1.05	2.05 ± 0.18	13.23 ± 2.01↑	12.21 ± 1.05↑	19.55 ± 2.01↑
60 mg%	18.76 ± 1.78	10.34 ± 0.98	13.85 ± 0.88	2.74 ± 0.31	5.23 ± 0.55	11.22 ± 0.67
80 mg%	24.72 ± 2.01	34.13 ± 2.02	40.13 ± 3.11	39.11 ± 2.11	44.33 ± 3.02	41.19 ± 2.67
<i>T. catappa</i> residual aqueous						
40 mg%	17.69 ± 1.6↑	22.80 ± 1.01↑	23.82 ± 1.2↑	15.83 ± 0.78↑	42.94 ± 3.18↑	46.95 ± 3.55↑
60 mg%	9.91 ± 1.03	7.39 ± 0.98	3.07 ± 0.56	5.91 ± 0.76	32.43 ± 3.67↑	56.38 ± 4.01↑
80 mg%	2.19 ± 0.86	17.09 ± 1.56	13.51 ± 1.11	17.61 ± 1.14	22.17 ± 1.45↑	53.56 ± 3.86↑

The results are mean (X) ± S.D of three (n = 3) determinations; mg% = mg/100 mL
 †: Activation of poly-dHbS-M

of fractionated leaf extracts of *A. occidentale*, *P. guajava*, and *T. catappa*. Within the experimental time range of 0 s ≤ t ≤ 180 s, 60 mg/100 mL petroleum ether extract of *A. occidentale* caused an increasing level of inhibition of poly-dHbS-M as the experimental time progressed. Table 2 showed that 40 and 80 mg/100 mL petroleum ether extracts of *A. occidentale* inhibited poly-dHbS-M at t < 90 s and t < 120 s respectively. Further increase in the experimental time showed that 40 and 60 mg/100 mL petroleum ether extracts of *A. occidentale* activated poly-dHbS-M. Among the three concentrations of petroleum ether extracts of *A. occidentale*, that of 60 mg/100 mL concentration exhibited the highest capacity to inhibit poly-dHbS-M; specifically at t = 180 s; inhibition of poly-dHbS-M = 18.65 ± 1.10% (Table 2).

The capacity of 40 mg/100 mL *n*-hexane extract to inhibit poly-dHbS-M ranged between 2.96 ± 0.03% at t = 90 s and 18.15 ± 1.21% at t = 60 s (Table 2). Similarly, 60 mg/100 mL *n*-hexane extract of *A. occidentale* inhibited poly-dHbS-M within the range of 7.04 ± 1.16% at t = 90 s and 25.19 ± 2.56% at t = 60 s. The highest capacity of *n*-hexane extract of *A. occidentale* to inhibit poly-dHbS-M was registered in the presence of 80 mg/100 mL of the extract, which corresponded to 27.41 ± 2.98% at t = 90 s. Conversely, 40 and 60 mg/100 mL *n*-hexane extracts of *A. occidentale* activated poly-dHbS-M at t > 90

s, whereas 80 mg/100 mL *n*-hexane extract of *A. occidentale* activated poly-dHbS-M at t = 180 s; activation of poly-dHbS-M was 9.26 ± 1.67% (Table 2).

Within the experimental time, 40 and 60 mg/100 mL chloroform extracts of *A. occidentale* activated poly-dHbS-M and were in the range of 31.25 ± 2.2–87.80 ± 4.90% and 17.55 ± 1.1–31.67 ± 3.0% respectively. Additionally, at t < 60 s, 80 mg/100 mL chloroform extract of *A. occidentale* activated poly-dHbS-M. Further increase in experimental time, t > 60 s, 80 mg/100 mL chloroform extract of *A. occidentale* inhibited poly-dHbS-M in the range of 27.38 ± 2.56–46.43 ± 3.56% (Table 2).

Table 2 showed that 40 and 60 mg/100 mL ethylacetate extracts of *A. occidentale* inhibited poly-dHbS-M within the experimental time. The 80 mg/100 mL ethylacetate extract inhibited poly-dHbS-M at t < 60 s, whereas further increase in experimental time, t > 60 s, caused activation of poly-dHbS-M in the range of 5.18 ± 1.01–31.85 ± 2.5%.

Table 2 showed that 40 mg/100 mL residue aqueous extract of *A. occidentale* exhibited decreasing capacity to activate poly-dHbS-M. At t = 180 s, 40 mg/100 mL residual aqueous extract of *A. occidentale* inhibited poly-dHbS-M by 29.93 ± 2.78%. Furthermore, 60 and 80 mg/100 mL residual aqueous extracts of *A. occidentale*

inhibited poly-dHbS-M at $t > 150$ s and $t > 120$ s respectively. Polymerization of deoxygenated sickle hemoglobin molecules (poly-dHbS-M) was activated in the presence of 40, 60, and 80 mg/100 mL petroleum ether extracts of *P. guajava* within the experimental time. Specifically, the stated concentrations of petroleum ether extracts of *P. guajava* activated poly-dHbS-M in the following corresponding range of values: (40 mg/100 mL) 56.25 ± 4.97 – $103.27 \pm 7.4\%$, (60 mg/100 mL) 51.48 ± 3.87 – $75.30 \pm 3.77\%$, and (80 mg/100 mL) 40.48 ± 3.32 – $75.16 \pm 3.78\%$ (Table 2).

The *n*-hexane extract of *P. guajava* inhibited poly-dHbS-M in a concentration-depended manner as the experimental time progressed. Table 2 showed that 40 mg/100 mL *n*-hexane extract of *P. guajava* exhibited a decreasing capacity to inhibit poly-dHbS-M, whereas 80 mg/100 mL *n*-hexane extract of *P. guajava* showed increasing capacity to inhibit poly-dHbS-M with increasing experimental time. The capacity of 40 mg/100 mL *n*-hexane extract of *P. guajava* to inhibit poly-dHbS-M peaked at $t = 30$ s; inhibition of poly-dHbS-M was $38.68 \pm 2.98\%$. Peak inhibition in the presence of 80 mg/100 mL *n*-hexane extract of *P. guajava* was at $t = 180$ s; inhibition of poly-dHbS-M was $51.73 \pm 4.03\%$, whereas that of 60 mg/100 mL of the extract was at $t = 180$ s; inhibition of poly-dHbS-M was $34.53 \pm 2.33\%$ (Table 2).

The chloroform extract of *P. guajava* activated poly-dHbS-M at $t = 30$ s. However, as the experimental time progressed, $t > 30$ s, the chloroform extract of *P. guajava* inhibited poly-dHbS-M in a time-dependent manner. Specifically, Table 2 showed that 80 mg/100 mL chloroform extract caused the highest inhibition ($38.84 \pm 2.78\%$) against poly-dHbS-M.

Table 2 showed that ethylacetate extract of *P. guajava* exhibited the highest capacity to inhibit poly-dHbS-M among the three ethylacetate extract concentrations. Conversely, poly-dHbS-M was activated by 60 mg/100 mL ethylacetate extract of *P. guajava* throughout the experimental time. Poly-dHbS-M was inhibited by 80 mg/100 mL of ethylacetate extract of *P. guajava* within the range of 9.93 ± 1.02 – $37.00 \pm 3.09\%$ (Table 2).

Table 2 showed that 40 and 60 mg/100 mL residual aqueous extracts of *P. guajava* inhibited poly-dHbS-M within the time range of $0 \leq t \leq 120$ s. Further increase in the experimental time, $t > 120$ s, 40, and 60 mg/100 mL residual aqueous extracts of *P. guajava* activated poly-dHbS-M in a concentration-depended manner (Table 2). Notably, 80 mg/100 mL residual aqueous extract of *P. guajava* caused activation of dHbS-M throughout the experimental time. Peak activation of poly-dHbS-M ($143.88 \pm 9.8\%$) occurred at $t = 180$ s in the presence of residual aqueous extract of *P. guajava* (Table 2).

Table 2 showed that 40, 60, and 80 mg/100 mL petroleum ether extracts of *T. catappa* caused activation of

poly-dHbS-M within the experimental time range of $0 \leq t \leq 120$ s. Peak activation of poly-dHbS-M ($57.07 \pm 4.78\%$) was registered in the presence of 60 mg/100 mL petroleum ether extract of *T. catappa* at $t = 60$ s. Further increase in experimental time, $t > 120$ s, showed that 60 and 80 mg/100 mL petroleum ether extracts of *T. catappa* inhibited poly-dHbS-M in a time-depended manner. However, 40 mg/100 mL petroleum ether extract of *T. catappa* activated poly-dHbS-M throughout the experimental time.

Within the experimental time, $t < 60$ s, 40, 60, and 80 mg/100 mL *n*-hexane extracts of *T. catappa* activated poly-dHbS-M (Table 2). Notably, 80 mg/100 mL *n*-hexane extract of *T. catappa* caused maximum activation of poly-dHbS-M at $t = 60$ s; activation of poly-dHbS-M was $19.16 \pm 1.56\%$. Conversely, Table 2 showed that 40 and 60 mg/100 mL *n*-hexane extracts of *T. catappa* inhibited poly-dHbS-M, whereas 80 mg/100 mL *n*-hexane extract caused activation at $t = 90$ s. Further increase in the experimental time caused inhibition of poly-dHbS-M by 40, 60, and 80 mg/100 mL *n*-hexane extracts of *T. catappa*. Peak inhibition of poly-dHbS-M (18.3 ± 1.2 %) by 60 mg/100 mL of *n*-hexane extract of *T. catappa* occurred at $t = 120$ s.

A cursory look at Table 2 showed that peak inhibition of poly-dHbS-M by 40, 60, and 80 mg/100 mL chloroform extracts of *T. catappa* occurred at $t = 60$ s, specifically, $0.98 \pm 0.02\%$, $11.13 \pm 1.78\%$, and $16.02 \pm 1.98\%$ respectively. Further increase in experimental time, $t > 60$ s, showed diminishing capacity of the extract to inhibit poly-dHbS-M. Additionally, 40 mg/100 mL chloroform extract of *T. catappa* activated poly-dHbS-M except at $t = 60$ s and $t = 120$ s.

Table 2 showed that 60 and 80 mg/100 mL ethylacetate extracts of *T. catappa* inhibited poly-dHbS-M within the experimental time with peak value at $t = 30$ s; inhibition of polymerization was $18.76 \pm 1.78\%$ and at $t = 90$ s; inhibition of polymerization was $40.13 \pm 3.11\%$ respectively. However, 40 mg/100 mL ethylacetate extract of *T. catappa* inhibited poly-dHbS-M within the experimental time; at $t < 90$ s. Further increase in experimental time caused activation of poly-dHbS-M by 40 mg/100 mL ethylacetate extract of *T. catappa* (Table 2).

At the given experimental time range of $0 \leq t \leq 180$ s, 40 mg/100 mL residue aqueous extract of *T. catappa* activated poly-dHbS-M with a peak value at $t = 180$ s; activation of poly-dHbS-M was $46.92 \pm 3.55\%$ (Table 2). Conversely, 60 and 80 mg/100 mL residual aqueous extracts of *T. catappa* inhibited poly-dHbS-M within the experimental time of $t < 120$ s. Further increase in experimental time caused activation of poly-dHbS-M (Table 2).

RCPI% of dHbS-M in the presence of fractionated leaf extracts

Table 3 showed the RCPI% of dHbS-M in the presence of fractionated leaf extracts of *A. occidentale*, *P. guajava*,

Table 3 Cumulative inhibition/activation of poly-dHbS-M by fractionated leaf extracts of *A. occidentale*, *P. guajava*, and *T. catappa*

Extract fraction	AUC $\times 10^3$ (%.second)/RCPI (%)			
	Control	40 mg%	60 mg%	80 mg%
<i>A. occidentale</i>				
Petroleum ether	15.12 \pm 2.08 ^a (100)	14.54 \pm 2.57 ^{a,b} (3.8)	13.09 \pm 8.32 ^{c,d} (13.4)	13.51 \pm 6.53 ^{a,b,c} (10.7)
<i>n</i> -hexane	22.21 \pm 1.48 ^{a,b} (100)	23.29 \pm 10.33 ^a (4.9) \uparrow	21.97 \pm 11.34 ^{a,b,c} (1.1)	20.17 \pm 9.61 ^{c,d} (9.2)
Chloroform	22.36 \pm 2.02 ^c (100)	30.54 \pm 16.59 ^a (36.6) \uparrow	26.71 \pm 7.09 ^{a,b} (19.5) \uparrow	19.44 \pm 7.17 ^d (13.1)
Ethylacetate	22.21 \pm 1.48 ^{a,b} (100)	9.02 \pm 5.54 ^d (59.4)	13.33 \pm 4.39 ^c (40.0)	23.18 \pm 14.34 ^a (4.4) \uparrow
Residual aqueous	16.65 \pm 2.00 ^d (100)	31.65 \pm 9.00 ^c (90.1) \uparrow	93.78 \pm 6.35 ^a (463.2) \ddagger	52.12 \pm 19.87 ^b (213.0) \ddagger
<i>P. guajava</i>				
Petroleum ether	22.36 \pm 2.02 ^d (100)	34.53 \pm 14.00 ^a (54.4) \uparrow	32.83 \pm 12.82 ^{a,b} (46.8) \uparrow	31.62 \pm 16.78 ^{a,b,c} (41.4) \uparrow
<i>n</i> -hexane	15.12 \pm 2.08 ^a (100)	9.69 \pm 4.00 ^{b,c} (35.9)	10.99 \pm 3.10 ^b (27.3)	8.98 \pm 2.24 ^{b,c,d} (40.6)
Chloroform	15.12 \pm 2.08 ^a (100)	13.56 \pm 1.45 ^{b,c} (10.3)	13.05 \pm 9.63 ^{b,c,d} (13.7)	13.77 \pm 2.94 ^b (8.9)
Ethylacetate	15.12 \pm 2.08 ^b (100)	9.86 \pm 3.69 ^{c,d} (34.8)	16.74 \pm 10.00 ^a (10.7) \uparrow	10.99 \pm 3.14 ^c (27.3)
Residual aqueous	16.65 \pm 2.00 ^c (100)	16.49 \pm 3.26 ^{c,d} (1.0)	19.09 \pm 3.95 ^b (14.7) \uparrow	23.87 \pm 1.35 ^a (43.4) \uparrow
<i>T. catappa</i>				
Petroleum ether	12.53 \pm 2.11 ^{c,d} (100)	16.36 \pm 5.88 ^{a,b} (30.6) \uparrow	16.51 \pm 5.07 ^a (31.8) \uparrow	13.32 \pm 3.25 ^c (6.3) \uparrow
<i>n</i> -hexane	13.85 \pm 5.93 ^{a,b} (100)	13.40 \pm 5.29 ^{a,b,c} (3.3)	13.00 \pm 6.80 ^{a,b,c,d} (6.1)	14.03 \pm 1.09 ^a (1.3) \uparrow
Chloroform	13.85 \pm 5.92 ^{a,b} (100)	14.37 \pm 2.02 ^a (3.8) \uparrow	13.53 \pm 2.00 ^{a,b,c} (2.3)	12.81 \pm 1.98 ^{c,d} (7.5)
Ethylacetate	13.85 \pm 5.92 ^{a,b} (100)	14.52 \pm 1.32 ^a (4.8) \uparrow	12.18 \pm 3.48 ^c (12.1)	7.78 \pm 2.12 ^d (43.8)
Residual aqueous	16.65 \pm 2.00 ^{b,c} (100)	21.05 \pm 1.08 ^a (26.4) \uparrow	17.68 \pm 6.75 ^b (6.2) \uparrow	16.61 \pm 5.00 ^{b,c,d} (0.2)

The mean (\bar{X}) \pm S.D of three ($n = 3$) determinations; mg% = mg/100 mL. Means in the row with the same letter are not significantly different at $p > 0.05$ according to LSD

\uparrow : Cumulative activation of poly-dHbS-M

\ddagger : RCPI%_{Test} > RCPI%_{Control}

and *T. catappa*. The RCPI% of dHbS-M in the presence of fractionated leaf extract of *A. occidentale* varied within a wide range of 3.8–59.4% and was indicative of cumulative inhibition of poly-dHbS-M. Conversely, in the presence of 40 mg/100 mL residual aqueous extract of *A. occidentale*, RCPI% was indicative of cumulative activation of poly-dHbS-M. Table 3 showed that RCPI% of dHbS-M in the presence 60 and 80 mg/100 mL residual aqueous extracts of *A. occidentale* were comparatively greater than that of the control sample. The RCPI% of dHbS-M of the samples containing 40, 60, and 80 mg/100 mL petroleum ether extracts of *P. guajava* as well as 80 mg/100 mL residual aqueous extract of *P. guajava* were indicative of cumulative activation of poly-dHbS-M (Table 3). Additionally, the comparative raised level of RCPI% of dHbS-M in the presence of 80 mg/100 mL *n*-hexane of *P. guajava* was indicative of higher capacity of the extract to cumulatively inhibit poly-dHbS-M than other concentrations of fractionated leaf extracts of *P. guajava*.

Table 3 showed that dHbS-M of the samples containing 60 and 80 mg/100 mL ethylacetate of *T. catappa* gave comparative raised levels of RCPI% indicative of cumulative inhibition of poly-dHbS-M. RCPI% of dHbS-M in the presence of 40 and 60 mg/100 mL petroleum ether extracts of *T. catappa* as well as 40 mg/100 mL

residual aqueous extract of *T. catappa* were indicative of comparatively raised levels of cumulative activation of poly-dHbS-M.

The dHbS-M of the sample containing 40 mg/100 mL residual aqueous of *A. occidentale* gave RCPI% = 90.1, which represented the maximum cumulative activation of poly-dHbS-M compared with other concentrations of fractionated leaf extracts of *A. occidentale*, *P. guajava*, and *T. catappa*.

The fractionated leaf extracts of *A. occidentale*, *P. guajava*, and *T. catappa* that exhibited comparatively high potency to inhibit poly-dHbS-M, summarized from Tables 2 and 3, were as follows: *A. occidentale* (petroleum ether and ethylacetate extracts), *P. guajava* (*n*-hexane, chloroform, and ethylacetate extracts), and *T. catappa* (ethylacetate extract).

Gas chromatograms of fractionated leaf extracts

The gas chromatograms, indicating the peaks of eluted phytochemicals at corresponding time intervals, of the fractionated leaf extracts of *A. occidentale*, *P. guajava*, and *T. catappa* that exhibited comparatively high potency to inhibit poly-dHbS-M are illustrated in Fig. 4a–f.

Table 4(A–F) showed the combinations of phytochemicals from fractionated leaf extracts of *A. occidentale*, *P. guajava*, and *T. catappa* denoting their retention

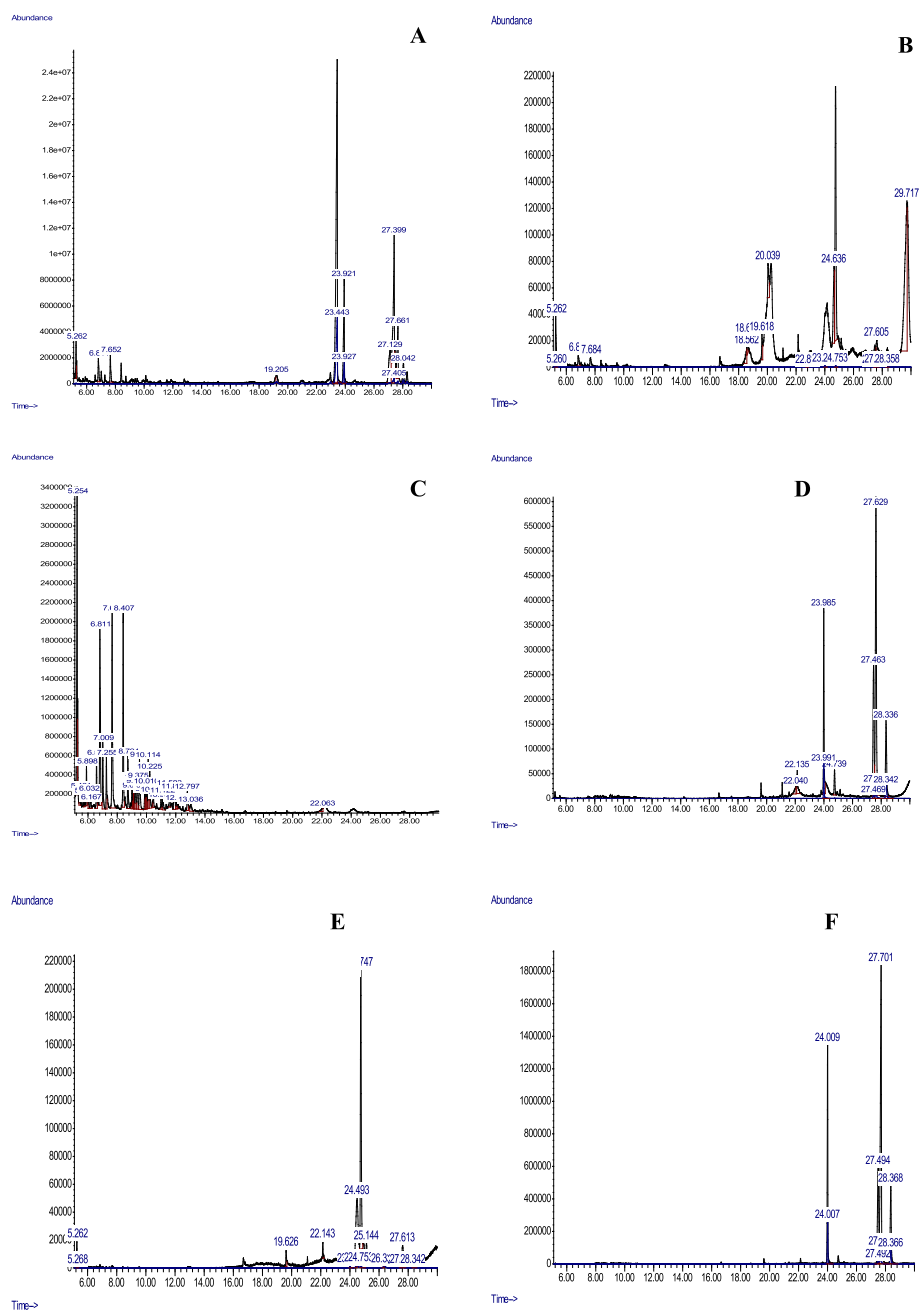


Fig. 4 GC-MS chromatograms. **a** Petroleum ether extract of *A. occidentale*. **b** Ethylacetate extract of *A. occidentale*. **c** *n*-Hexane extract of *P. guajava*. **d** Chloroform extract of *P. guajava*. **e** Ethylacetate extract of *P. guajava*. **f** Ethylacetate extract of *T. catappa*

time, molecular formula, and weights as well as their relative abundance denoted as percentage of peak areas (%PA) of the chromatograms. Also, the presence of aliphatic compounds in corresponding fractionated leaf extracts of *A. occidentale*, *P. guajava*, and *T. catappa* are summarized in Table 4(A–F).

In comparative terms, Table 4(A) showed that the major phytochemicals from petroleum ether extract of *A. occidentale* were hexadecanoic acid, methyl ester, 11-

octadecenoic acid, and pentadecanoic acid-14-methyl, methyl ester. Likewise, pentacosane, dibutyl phthalate, and tricosane were the major phytochemicals from ethylacetate extract of *A. occidentale* (Table 4(B)). D-Erythro-sphinganine was the phytochemical detected in appreciable quantity in *n*-hexane extract of *P. guajava* (Table 4(C)). Additionally, the major phytochemicals from chloroform extract of *P. guajava* were 11-octadecenoic acid, methyl ester, 9,11-octadecadienoic

Table 4 Phytocomponents of (A) petroleum ether extract of *A. occidentale*, (B) ethylacetate extract of *A. occidentale*, (C) *n*-hexane extract of *P. guajava*, (D) chloroform extract of *P. guajava*, (E) ethylacetate extract of *P. guajava*, and (F) ethylacetate extract of *T. catappa*

S/No.	T_R (min)	Phytocomponents	MF	MW (g/mol)	%PA
A					
1.	5.262	<i>o</i> -Xylene	$C_6H_4(CH_3)_2$	106.16	2.30
2.	6.811	Benzene, 1-ethyl-4-methyl-	C_9H_{12}	120.19	2.13
3.	7.652	Benzene, 1, 2, 4-trimethyl-	C_9H_{12}	120.19	2.33
4.	19.205	Methyl tetradecanoate ^P	$C_{15}H_{30}O_2$	242.40	1.53
5.	23.437	Hexadecanoic acid, methyl ester ^P	$C_{17}H_{34}O_2$	270.45	49.59
6.	23.921	Pentadecanoic acid, 14-methyl-, methyl ester ^P	$C_{17}H_{34}O_2$	270.50	10.34
7.	27.129	9, 12-Octadecadienoic acid (Z, Z)-, methyl ester ^P	$C_{19}H_{34}O_2$	294.47	8.49
8.	27.399	11-Octadecenoic acid, methyl ester ^P	$C_{19}H_{36}O_2$	296.49	14.14
9.	27.661	9-Octadecenoic acid, methyl ester, (E)- ^P	$C_{19}H_{36}O_2$	296.49	6.52
10.	28.042	Methyl stearate ^P	$C_{19}H_{38}O_2$	298.50	2.62
B					
1.	5.262	Benzene, 1, 3-dimethyl-	C_8H_{10}	106.17	3.97
2.	6.826	2, 4-Nonadiyne	C_9H_{12}	120.19	1.33
3.	7.684	Benzene, (1-methylethyl)-	C_9H_{12}	120.19	1.31
4.	18.562	Hexacosane ^P	$C_{26}H_{54}$	366.72	2.27
5.	18.617	Methoxyacetic acid, 3-pentadecyl ester ^P	$C_{18}H_{36}O_3$	300.50	1.71
6.	19.618	1-Hexacosanol ^P	$C_{26}H_{54}O$	382.70	2.38
7.	20.039	Tetracosane ^P	$C_{24}H_{50}$	338.70	4.66
8.	22.817	2-Hexyl-1-octanol ^P	$C_{14}H_{30}O$	214.39	< 0.01
9.	24.001	Diisooctyl phthalate ^P	$C_{24}H_{38}O_4$	390.60	< 0.01
10.	24.478	Bicyclo [4.1.0] heptane-3-cyclopropyl-7-hydroxymethyl [cis] ^P	$C_{11}H_{18}O$	166.26	< 0.01
11.	24.636	Tricosane ^P	$C_{23}H_{48}$	324.60	10.55
12.	24.747	Dibutyl phthalate ^P	$C_{16}H_{22}O_4$	278.34	29.34
13.	27.605	Undec-10-ynoic acid, undecyl ester ^P	$C_{22}H_{40}O_2$	336.55	1.53
14.	27.629	3-Cyclopentylpropanoic acid, but-3-yn-2-yl ester ^P	$C_{12}H_{18}O_2$	194.27	< 0.01
15.	28.360	4-Nonanol 2, 6, 8 trimethyl- ^P	$C_{12}H_{26}O$	186.33	< 0.01
16.	29.717	Pentacosane ^P	$C_{25}H_{52}$	352.70	40.95
C					
1.	25.001	D-Erythro-sphinganine ^P	$C_{18}H_{39}NO_2$	525.00	< 0.01
D					
1.	22.040	Ethanol, 2-(dodecyloxy)- ^P	$C_{14}H_{30}O_2$	230.39	1.46
2.	22.135	Tricosyl heptafluorobutyrate ^P	$C_{27}H_{47}F_7O_2$	536.65	2.79
3.	23.993	Hexadecanoic acid, methyl ester ^P	$C_{17}H_{34}O_2$	270.45	5.63
4.	24.739	Dibutyl phthalate ^P	$C_{16}H_{22}O_4$	278.34	2.85
5.	27.463	9, 11-Octadecadienoic acid, methyl ester, (E,E)- ^P	$C_{19}H_{34}O_2$	294.47	19.52
6.	27.471	9, 12-Octadecadienoic acid [Z, Z], methyl ester ^P	$C_{19}H_{34}O_2$	294.47	5.64
7.	27.637	Trans-13-octadecenoic acid, methyl ester ^P	$C_{19}H_{36}O_2$	296.49	5.62
8.	27.629	11-Octadecenoic acid, methyl ester ^P	$C_{19}H_{36}O_2$	296.49	44.49
9.	28.336	Methyl stearate ^P	$C_{19}H_{38}O_2$	298.50	12.00
E					
1.	5.262	Benzene, 1, 3-dimethyl-	C_8H_{10}	106.17	4.30

Table 4 Phytocomponents of (A) petroleum ether extract of *A. occidentale*, (B) ethylacetate extract of *A. occidentale*, (C) *n*-hexane extract of *P. guajava*, (D) chloroform extract of *P. guajava*, (E) ethylacetate extract of *P. guajava*, and (F) ethylacetate extract of *T. catappa* (Continued)

S/No.	T_R (min)	Phytocomponents	MF	MW (g/mol)	%PA
2.	5.270	p-Xylene	C ₈ H ₁₀	106.16	< 0.01
3.	19.626	2-Tetradecanol ^P	C ₁₄ H ₃₀ O	214.39	2.46
4.	22.143	5-Octadecene, (E)-	C ₁₈ H ₃₆	252.48	1.91
5.	24.001	Heptanoic acid, 3, 6, 6-trimethyl-methyl ester ^P	C ₁₁ H ₂₂ O ₂	186.29	< 0.01
6.	24.485	Methyl 12-hydroxy-9-octadecenoate ^P	C ₁₉ H ₃₆ O ₃	312.50	< 0.01
7.	24.493	9-Octadecenoic acid, 12-hydroxy-, methyl ester, [R-(Z)]- ^P	C ₁₉ H ₃₆ O ₃	312.49	29.32
8.	24.747	Dibutyl phthalate ^P	C ₁₆ H ₂₂ O ₄	278.34	56.52
9.	25.144	1-Dodecanol, 2-octyl- ^P	C ₂₀ H ₄₂ O	298.50	2.90
10.	26.335	Oxiraneundecanoic acid, 3-pentyl-, methyl ester, cis ^P	C ₁₉ H ₃₆ O ₃	312.50	< 0.01
11.	27.470	1, 2-Cyclohexanediol, cyclic sulfite, cis ^P	C ₆ H ₁₀ O ₃ S	162.21	< 0.01
12.	27.613	9-Octadecenoic acid (Z)-, methyl ester ^P	C ₁₉ H ₃₆ O ₂	296.49	2.59
13.	27.621	1-Eicosanol ^P	C ₂₀ H ₄₂ O	298.50	< 0.01
14.	28.344	Methyl phosphonic acid, ethyl ester ^P	C ₃ H ₉ O ₃ P	124.08	< 0.01
F					
1.	24.009	Hexadecanoic acid, methyl ester ^P	C ₁₇ H ₃₄ O ₂	270.45	20.03
2.	27.494	9, 11-Octadecadienoic acid, methyl ester, (E, E)- ^P	C ₁₉ H ₃₄ O ₂	294.50	18.26
3.	27.701	Trans-13-octadecenoic acid, methyl ester ^P	C ₁₉ H ₃₆ O ₂	296.49	49.49
4.	28.368	Methyl stearate ^P	C ₁₉ H ₃₈ O ₂	298.50	12.22

T_R retention time, MF molecular formula, MW molecular weight, PA peak area, %PA < 0.01 trace Amount (Sampaio et al. 2011), ^P plant metabolite

acid, methyl ester, (E, E), and methyl stearate (Table 4(D)). Table 4(E) showed that the relative abundance of dibutyl phthalate and 9-octadecenoic acid-12-hydroxy-, methyl ester, [R-(Z)]- in ethylacetate extract of *P. guajava* was equivalent to 56.52 %PA and 29.32 %PA respectively. Ethylacetate extract of *T. catappa* contained four phytocomponents and their relative abundance equivalent to %PA ranged between 12.22 and 49.49 (Table 4(F)).

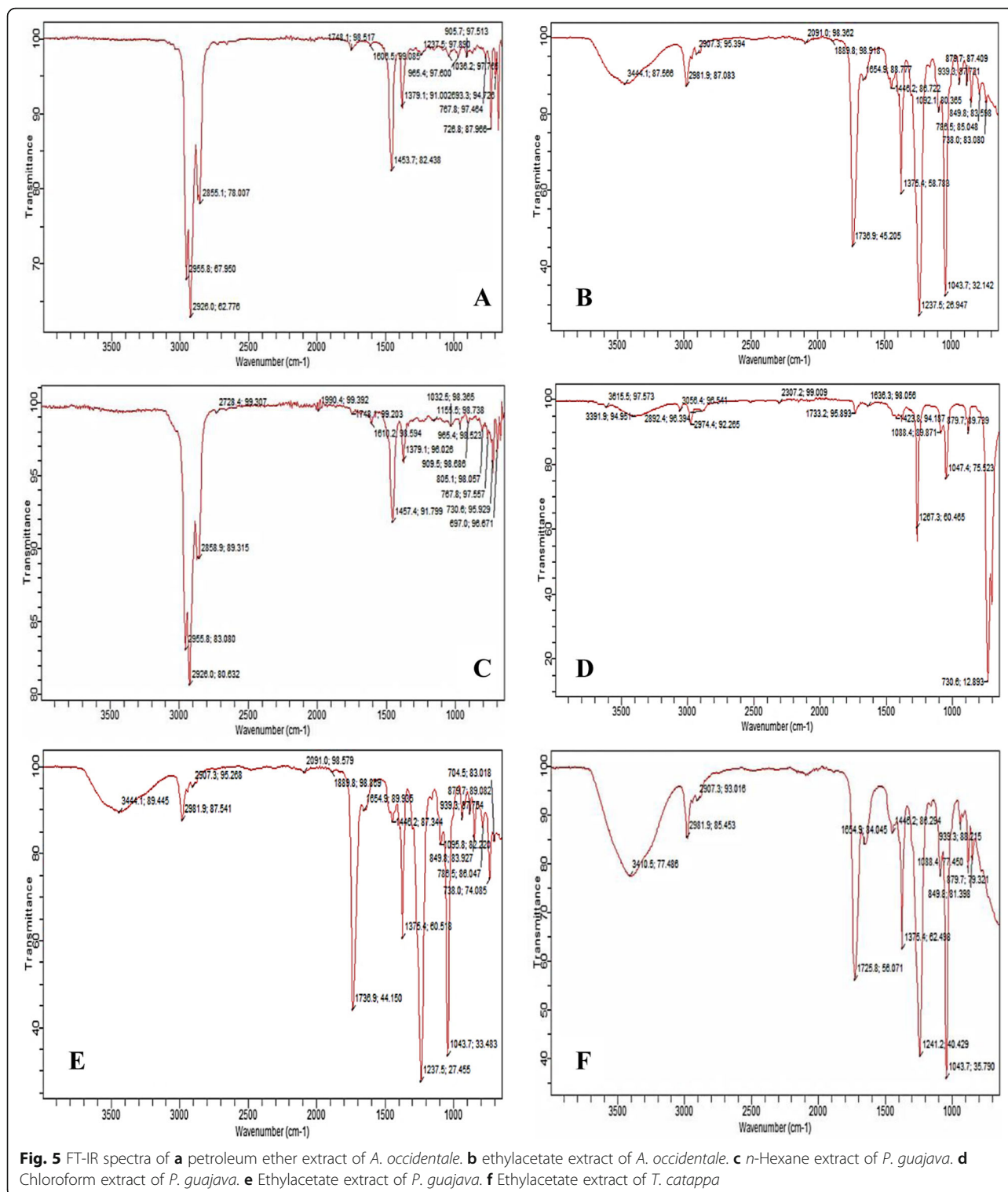
FT-IR spectra of fractionated leaf extracts

Figure 5a–f showed FT-IR spectra of *A. occidentale* (petroleum ether and ethylacetate extracts), *P. guajava* (*n*-hexane, chloroform, and ethylacetate extracts), and *T. catappa* (ethylacetate extract) and summarized in Table 4(A–F). Petroleum ether extract of *A. occidentale* gave characteristic peaks depicting sp³ C-H stretch within the range of 2955.8–2926.0 cm⁻¹ (Table 4(A)). The C-H stretch at 2855.1 cm⁻¹ exhibited medium band and C-O stretch at 1748.1 cm⁻¹ exhibited weak band, which were indicative of the presence of molecular species containing aldehyde (HC=O) and ester carbonyl (C=O) functional groups. Additionally, ether C-O stretch at 1036.2 cm⁻¹ suggested the presence of alkoxy (X-O-C) functional group in petroleum ether extract of *A. occidentale*. The presence of conjugated alkenes in petroleum ether extract of *A. occidentale* was indicative of weak band at 1606.5 cm⁻¹ and medium band at 1453.7 cm⁻¹ were indicative of aromatic compound C=C

stretch (Fig. 5a). Petroleum ether extract of *A. occidentale* exhibited characteristic peaks within the range of (905.7–693.3) cm⁻¹, suggesting the presence of aromatic compounds in the fraction. The peaks at 1379.4 cm⁻¹ and 1237.5 cm⁻¹ indicated the presence of nitro-compounds and halide containing organic compounds (Table 4(A)).

Figure 5b showed that ethylacetate extract of *A. occidentale* exhibited characteristic broad band around 3444.1 cm⁻¹, which was indicative of the presence of dimeric alcohol functional group (O-H) stretch (Table 4(B)). The fraction also exhibited alkanes sp³ (-C-H) stretch within the region of (2989.1–2907.3) cm⁻¹ and alkenes sp² (=C-H) bend at (939.3–878.7) cm⁻¹. Likewise, Fig. 5b showed peak values within the range of (939.3–849.8) cm⁻¹, which were indicative of the presence of unsaturated hydrocarbons, typified by alkenes sp² (=C-H) bend and tri-substituted alkenes (=C-H) bend. The C-O stretch within the regions of (1889.8–1654.9) cm⁻¹ and 1376.9 cm⁻¹ were indicative of the presence of carbonyl functional (C=O) and amide (H₂N-C=O) groups in ethylacetate extract of *A. occidentale* (Table 4(B)). Aromatic compounds in ethylacetate extract of *A. occidentale* exhibited C-H bend at regions of 786.5 and 733.0 cm⁻¹ (Table 4(B)).

Figure 5c showed that *n*-hexane extract of *P. guajava* exhibited alkanes sp³ (-C-H) stretch within the regions (2955.8–2858.9) cm⁻¹ as well as alkenes sp² C-H bend



and aromatic compound (=C-H) bend at (909.5–697.0) cm^{-1} regions, which were characteristically similar to that of petroleum ether extract of *A. occidentale*. However, *n*-hexane extract of *P. guajava* exhibited cyanate C-N stretch at 1990.4 cm^{-1} as well as aromatic

compound ring stretch at 1457.4 cm^{-1} (Table 4(C)). It is worthwhile to note that *n*-hexane extract of *P. guajava* exhibited characteristically distinct primary and tertiary amines (C-N) stretch within the regions of (1155.5–1032.5) cm^{-1} .

Chloroform extract of *P. guajava* contained aliphatic compounds such as primary amines, alkanes, alkenes, and alkynes as well as aromatic compounds. Peaks within the regions of 3391.9–3615.5 cm^{-1} suggested primary N-H stretch (Fig. 5d). Alkanes sp³ (-C-H) stretch, alkenes sp² (=C-H) stretch, and alkynes sp (\equiv C-H) stretch, which were within the regions of (3056.4–2307.2) cm^{-1} , were characteristic of chloroform extract of *P. guajava* (Table 4(D)). Peaks at 1733.2, 1636.3, and 1047.4 cm^{-1} were indicative of aldehyde (HC=O) stretch, amide (N-C=O) stretch, and alkoxy C-O stretch (Table 4(D)).

Figure 5e showed that ethylacetate extract of *P. guajava* exhibited characteristic alcohol (O-H) stretch at region of 3444.1 cm^{-1} as well as band patterns that suggested the presence of aliphatic compounds {2981.9 cm^{-1} (alkanes sp³ C-H stretch), 2091.0 cm^{-1} (alkynes sp C-H stretch), 878.7 cm^{-1} (alkenes sp² C-H bend), 849.8 cm^{-1} (tri-substituted alkenes sp² C-H bend), 785.5 cm^{-1} (*cis*-alkenes sp² C-H bend), 738.0–83.018 cm^{-1} (*cis*-alkenes sp² C-H bend)} (Table 4(E)). Ethylacetate extract of *P. guajava* showed evidence of the presence of carboxylic acids, aldehydes, phenolics, and esters, typified by peaks around 1889.8 cm^{-1} (C=O) stretch, 1736.9 cm^{-1} (HC=O) stretch, 1237.5 cm^{-1} acyl (C=O) stretch, and 1095.8 cm^{-1} alkoxy (C-O-R) stretch respectively. Table 4(E) showed that ethylacetate extract of *P. guajava* contained aromatic and nitro- compounds.

Ethylacetate extract of *T. catappa* exhibited characteristic alcohol (O-H) stretch around 3410.5 cm^{-1} (Fig. 5f). Table 4(F) showed that ethylacetate extract of *T. catappa* contained aldehydes, aromatic and nitro- compounds, as well as phenolics and esters. Peaks around 2981.9 and 2907.0 cm^{-1} were evidence of the presence of aliphatic compounds in ethylacetate extract of *T. catappa*. Furthermore, medium band at 1043.7 cm^{-1} , typified by C-O stretch, was indicative of the presence of alkoxy group in ethylacetate extract of *T. catappa*. Peaks within the range of (939.3–849.8) cm^{-1} exhibited aliphatic sp² C-H bend, which was indicative of the presence of aliphatic compounds in ethylacetate extract of *T. catappa*.

UV-visible spectra of fractionated leaf extracts

Figure 6a–f showed characteristic patterns of UV-visible spectra of selected fractionated leaf extracts of *A. occidentale*, *P. guajava*, and *T. catappa*. The multiple λ_{max} of petroleum ether extract of *A. occidentale* was within the range of (224.00–272.00) nm, which suggested the presence of nitrite (-ONO) and nitrate (-NO₃) chromophores in the extract (Fig. 6a). Figure 6b showed no evidence of presence of chromophores, within the UV-visible spectra, in ethylacetate extract of *A. occidentale*. The *n*-hexane extract of *P. guajava* gave λ_{max} within the range of (248.00–281.00) nm (Fig. 6c), whereas that

of chloroform extract of *P. guajava* was between 200.00 and 281.00 nm (Fig. 6d). Ethylacetate extracts of *P. guajava* and *T. catappa* gave corresponding single λ_{max} at 217.00 nm (Fig. 6e) and 363.00 nm (Fig. 6f) respectively.

Discussion

The solid-liquid solvent extraction protocols are commonly used for the empirical evaluation of phytochemicals. The overall quality, phytochemical profile, and relative quantity (percentage yield) of plant extracts depend on a multitude of intrinsic elements such as age, species, and genetic constitution of the plant in addition to the plant parts of interest for empirical evaluation. The extrinsic factors include but not limited to growth conditions, geographical location, soil chemistry and seasonal period of the harvest of the plant materials (Mburu et al. 2012; Chikezie and Ojiako 2013; Mousavi et al. 2018). For the most part, the polarity of the solvent used in solid-liquid solvent extraction protocol has a bearing on the percentage yield of plant extracts (Mohd et al. 2012) composed of combinations of phytochemicals with diverse physical and chemical properties (Saxena et al. 2013). Furthermore, the phytochemical profile of fractionated extracts is intricately connected with the polarities of solvents of the partitioning cocktails as previously reported (Chikezie et al. 2015; Mousavi et al. 2018). Accordingly, fair insights into the physicochemical properties of the phytochemicals in a given plant material provide a guide for selecting the appropriate solvent for extraction protocol in order to achieve the maximum yield of their diverse phytochemicals. The present study showed variability in percentage yields of the fractionated leaf extracts of *A. occidentale*, *P. guajava*, and *T. catappa*, which contained combinations of phytochemicals of diverse biologic and chemical properties. The comparatively high yields of residual aqueous fractions of the plant materials suggested the presence of relatively high levels of hydrophilic phytochemicals in *A. occidentale*, *P. guajava*, and *T. catappa* leaf extracts. It is worthwhile to mention that hydrophilic and hydrophobic phytochemicals exhibit diverse biological activities, in which their ultimate pharmacological actions elicit therapeutic benefits or toxic outcomes (Chikezie et al. 2015).

HbS aggregation and polymerization are pivotal primary events leading to the distortion of sickle erythrocyte morphology and presentation of pathophysiologic indicators of SCD (Vekilov 2007; Uzunova et al. 2010; Piccin et al. 2019). In search of remedies for SCD, using *in vitro* models, previous empirical studies have demonstrated the capability of varieties of herbal extracts to control and impede HbS aggregation and polymerization (Okpuzor et al. 2008; Uwakwe and Nwaoguikpe 2008; Chikezie et al. 2010; Chikezie 2011; Imaga 2013; Dash

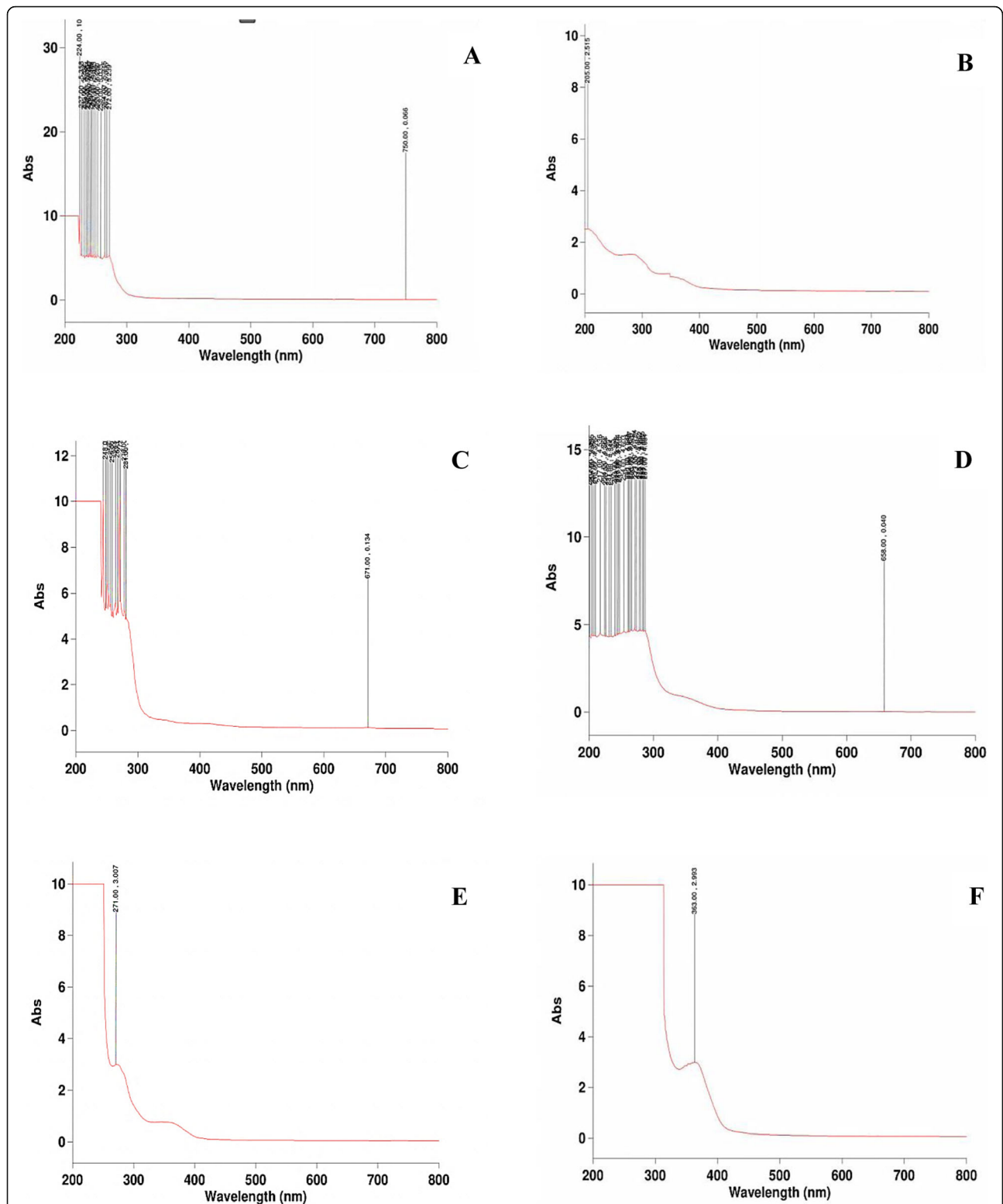


Fig. 6 UV-visible spectra. **a** Petroleum ether extract of *A. occidentale*. **b** Ethylacetate extract of *A. occidentale*. **c** *n*-Hexane extract of *P. guajava*. **d** Chloroform extract of *P. guajava*. **e** Ethylacetate extract of *P. guajava*. **f** Ethylacetate extract of *T. catappa*

et al. 2013; Pauline et al. 2013; Nurain et al. 2017). In concord with previous reports, the outcome of the present investigations showed that certain fractionated leaf extracts of *A. occidentale*, *P. guajava*, and *T. catappa* attenuated the tendency of HbS to aggregate and polymerize in vitro. Selected fractionated leaf extracts, namely petroleum ether and ethylacetate extracts of *A. occidentale*, *n*-hexane, chloroform, and ethylacetate extracts of *P. guajava*, as well as ethylacetate extract of *T. catappa*, contained phytochemicals that attenuated intermolecular aggregation of dHbS-M.

In the absence of impeding molecular species, from plant extract, against HbS aggregation and polymerization, several mechanisms have been ascribed to the tendencies of phytochemicals to attenuate HbS aggregation and polymerization (Chikezie 2011; Syed et al. 2019). Based on previous reports and reviews, the options available include one or combinations of the following mechanisms:

- i. The propensity of molecular species from plant extract to reversibly interact and interphase with complementary contact regions constituted by Val-beta6 residue of the docking dHbS-M and Leu-beta88, Phe-beta85, and Asp-beta73 residues of adjacent dHbS-M, and thereby, alters and shields the hydrophobic microenvironment of the contact regions required for HbS aggregation and polymerization (Chang et al. 1983; Charache et al. 1995; Abdulmalik et al. 2005; Eaton and Bunn 2017; Syed et al. 2019).
- ii. The molecular species from plant extract stabilize HbS molecule by reversible non-covalent interactions that thermodynamically favour R-state HbS (Manning and Acharya 1984; Kark et al. 1988; Oyewole et al. 2008; Safo and Kato 2014; Oder et al. 2016; Eaton and Bunn 2017).
- iii. Chemical modification of HbS molecule by molecular species from plant extract results in HbS derivatives that are adverse to aggregation and polymerization (Manning and Acharya 1984; Xu et al. 1999; Oder et al. 2016).

The major components of results of the present study appeared to suggest that reversible non-covalent interaction between phytochemicals from fractionated leaf extracts of *A. occidentale*, *P. guajava*, and *T. catappa* and HbS, for the most parts, was responsible for the capacities of the phytochemicals to attenuate HbS aggregation and polymerization. However, the non-covalent interaction may possibly wane as the experimental time progressed due to relatively transient nature of the interaction. Furthermore, two competing thermodynamic favorable interactions, namely dHbS-M...dHbS-M and dHbS-M...phytochemical interactions were responsible for the dual behaviors,

in certain instances (Tables 3 and 4), of phytochemicals from fractionated leaf extracts of *A. occidentale*, *P. guajava*, and *T. catappa* to either exacerbate or attenuate HbS aggregation and polymerization. Precisely, increased entropy kept the interacting species apart, whereas favorable free energy of intermolecular non-covalent interaction, measured by entropy gained, permitted the molecules to associate (Vekilov 2007; Syed et al. 2019). The molecular features of the interacting species and entropy of the interacting environment either exacerbated or attenuated HbS aggregation and polymerization. Accordingly, non-covalent interactions involving dHbS-M and phytochemicals may be disrupted and displaced by more thermodynamic favored interactions with the progression of time, whereby dHbS-M...dHbS-M interactions were favored fostering exacerbated HbS aggregation and polymerization or otherwise. Conversely, dHbS-M...phytochemical interactions may attenuate HbS aggregation and polymerization provided the molecular configuration of the microenvironment of the contact regions required for HbS aggregation and polymerization was such that negated dHbS-M...dHbS-M interactions but promoted dHbS-M...phytochemical interactions (Syed et al. 2019).

Another approach to deter HbS aggregation and polymerization involves the use of chemical agents that stabilize relax state (R-state) hemoglobin. The R-state HbS conformation is such that the contact regions required for HbS aggregation and polymerization are shielded, and as a result, do not form fibrous HbS polymers that engender erythrocyte sickling and ensuing clinical crisis (Safo and Kato 2014; Oder et al. 2016; Eaton and Bunn, 2017). It is remarkable to note that the presence of isothiocyanates in ethylacetate extract of *A. occidentale* obviously contributed, in parts, to impeding HbS aggregation and polymerization, which was in agreement with previous reports (Park et al. 2003; Safo and Kato 2014). Earlier reports showed that the thiols and isothiocyanates formed a covalent adduct with hemoglobin molecules, and thereby, modified the protein to an allosteric state of enhanced oxygen affinity that is adverse to polymerization (Park et al. 2003; Safo and Kato 2014). Specifically, studies showed that aliphatic isothiocyanates bound covalently to β^{93} cystine (Cys-beta93) disrupted the native T-state salt-bridge interaction between β^{94} aspartate (Asp-beta94) and β^{146} histidine (His-beta146), and thereby, destabilized the lower oxygen affinity T-state of HbS that promoted hemoglobin aggregation and polymerization (Safo and Kato 2014; Oder et al. 2016). R-state HbS does not polymerize, whereas T-state HbS forms fibrous polymer (Eaton and Hofrichter 1987).

Additionally, the previous report showed that isoquercitrin (quercetin-3-O- β -D-glucopyranoside) was one of the bioactive components from numerous medicinal

plants that readily interacted with HbS and, as a result, impeded HbS aggregation and polymerization (Syed et al. 2019). Using circular dichroism (CD) spectroscopy, Syed et al. (2019) revealed that HbS...isoquercitrin complex exhibited helical structural changes leading to destabilization of HbS polymer as previously described (Hamdani et al. 2009; Ding et al. 2012; Pauline et al. 2013) as well as stabilized R-state of HbS. Their findings were in agreement with the proposed mode of action of phytochemicals investigated in the present study. Accordingly, isothiocyanates from ethylacetate extract of *A. occidentale* were stabilizers of R-state of HbS in vitro as previously established (Park et al. 2003; Safo and Kato 2014).

Paradoxically, another selected fractionated leaf extracts of *A. occidentale*, *P. guajava*, and *T. catappa* were indicated to exacerbate HbS aggregation and polymerization (Tables 2 and 3), which was in concord with earlier reports (Chikezie et al. 2013). The present results suggest that these groups of fractionated leaf extracts of *A. occidentale*, *P. guajava*, and *T. catappa*, by virtue of their peculiar phytochemical profile, promoted HbS aggregation and polymerization. In a connected research outcome, Uzunova et al. (2010) had previously reported that the addition of 100–260 mM of free heme to dialyzed HbS solutions exacerbated HbS aggregation and polymerization by two orders of magnitude than before dialysis. They noted that the removal of free heme from HbS solutions by dialysis lowered HbS polymerization activity and further proposed that the prevention of free heme accumulation in the erythrocyte cytosol was a therapeutic strategy against SCD.

Chemical modification of HbS molecule by phytochemicals from plant extracts was probably the basis for the rapid and sustained exponential reversion of HbS aggregation and polymerization, typified by HbS polymerization in the presence of residual aqueous of *A. occidentale* (Fig. 1e). It implied, therefore, that the physicochemical properties of phytochemicals from the fractionated leaf extracts of *A. occidentale*, *P. guajava*, and *T. catappa* had direct bearing on their capacities to alter the process leading to HbS aggregation and polymerization. Since intra-erythrocytic HbS aggregation and polymerization are pivotal to the pathogenesis and pathophysiology of SCD (Uzunova et al. 2010; Piccin et al. 2019), the use of chemical agents that covalently modify HbS molecules has been suggested to be an important approach to impede dHbS-M aggregation and polymerization (Park et al. 2003; Eaton and Bunn 2017; Kassa et al. 2019). Covalent modification of HbS molecules by carbamylation using isothiocyanates, acetylation using methyl acetyl phosphate (MAP), and S-nitrosylation of Cys-beta93 has been reported (Xu et al. 1999; Park et al. 2003; Chikezie, 2011; Jana et al. 2018). Furthermore, 5-hydroxymethyl-2-furfural (5HMF) forms

a high-affinity Schiff-base adduct with HbS molecules, and thereby impede the tendency of dHbS-M to aggregate and polymerize (Abdulmalik et al. 2005; Safo and Kato, 2014; Oder et al. 2016; Eaton and Bunn, 2017).

However, synthetic covalent modifiers that interrupted HbS aggregation and polymerization might cause undesirable chemical modifications of HbS molecules and other body protein molecules due to their non-specific chemical reactions (Safo and Kato 2014; Eaton and Bunn 2017). Although there are envisaged challenges in applying these options in the management of SCD as a result of a lack of stereo-specificity in dHbS-M...phytochemicals interactions at the complementary contact regions or allosteric sites of dHbS-M, this approach still offers rewarding prospects for alleviation of the sickling phenomena and therefore should not be discounted (Eaton and Bunn 2017).

The present study gave molecular insights into the identities of phytochemicals from fractionated leaf extracts of *A. occidentale*, *P. guajava*, and *T. catappa* that attenuated HbS aggregation and polymerization within the experimental time of 180 s. The molecular features of the phytochemicals implicated in this regard, revealed by GC-MS and FT-IR systems analyses, were the aliphatic hydrocarbons, methylated esters, methylated long-chain and short-chain fatty acids, volatile alkanes, short-chain aliphatic alcohols, aromatic derivatives, cycloalkanes, phthalates, isothiocyanates, aminated sugars, cyclo-alcohols, and arachidyl alcohols (Tables 4(A–F) and Table 5(A–F)). Furthermore, UV-visible investigations revealed the presence of nitro-compounds in petroleum ether extract of *A. occidentale* as a phytochemical that attenuated HbS aggregation and polymerization (Fig. 6v).

The present study showed that *n*-hexane extract of *P. guajava* exhibited the highest capacity to attenuate HbS aggregation and polymerization compared to other fractionated extracts of *A. occidentale*, *P. guajava*, and *T. catappa*. A combined result of GC-MS and FT-IR protocols showed that the phytochemicals from *P. guajava* that attenuated HbS aggregation and polymerization were viz. D-erythro-sphinganine, nitro compounds, tertiary amine, primary amine, di-, tri-substituted aromatic compounds, cyanate, and esters.

The present study further confirmed the usefulness of GC-MS systems in identification, quantification, and characterization of a mixture of phytochemicals with commensurate reproducibility and reliable outcomes. Accordingly, the application of GC-MS systems protocols, which unravel the nature, quantity, and chemical structures as well as molecular fingerprints of the vast array of phytochemicals from biologic systems have been widely reported (Sasidharan et al. 2011; Sampaio et al. 2011; Rašković et al. 2015; Cyril-Olutayo et al. 2019). To mention but a few, the findings of the present

Table 5 FT-IR spectra peak values of (A) petroleum ether extract of *A. occidentale*, (B) ethylacetate extract of *A. occidentale*, (C) *n*-hexane extract of *P. guajava*, (D) chloroform extract of *P. guajava*, (E) ethylacetate extract of *P. guajava*, and (F) ethylacetate extract of *T. catappa*

S/No	Peak/band (cm ⁻¹)	%T	Functional groups/assignment	Origin
A				
1.	2955.8	67.950	Alkanes sp ³ C-H stretch	C-H
2.	2926.0	62.776	Alkanes sp ³ C-H stretch	C-H
3.	2855.1	78.007	Aldehyde C-H stretch	C-H
4.	1748.1	98.517	Ester carbonyl C-O stretch	C=O
5.	1606.5	99.085	Conjugated alkenes C-C	C=C
6.	1453.7	82.438	Aromatic compounds C-C stretch	C=C
7.	1379.4	91.002	Acyl C-O; phenol C-O stretch	C=O; C-O
8.	1237.5	97.513	Aromatic ethers, aryl-O stretch	Ar-O-C
9.	1036.2	97.765	Alkoxy C-O stretch	X-O-C
10.	905.7	97.513	Mono-substituted alkene sp ² C-H bend	=C-H
11.	767.8	97.464	Di-substituted aromatic sp ² C-H bend	=C-H
12.	726.8	87.966	Mono-substituted aromatic sp ² C-H bend	=C-H
13.	693.3	94.726	Di-substituted aromatic sp ² C-H bend	=C-H
B				
1.	3444.1	87.566	Dimeric O-H stretch	O-H
2.	2989.1	87.083	Alkanes sp ³ C-H stretch	C-H
3.	2907.3	95.394	Alkanes sp ³ C-H stretch	C-H
4.	2091.0	98.362	Isothiocyanate (-SCN) stretch	-SCN
5.	1889.8	98.918	Carboxylic acids C-O stretch	C=O
6.	1736.9	45.205	Ester C-O stretch	C=O
7.	1654.9	88.777	Amides C-O stretch	C=O
8.	1446.2	86.722	Aromatic compounds C-C stretch	C=C
9.	1376.9	45.205	Acyl C-O; phenol C-O stretch	C=O; C-O
10.	1237.5	26.947	Skeletal C-C vibration	C-C
11.	1092.1	80.365	Alkoxy C-O stretch	X-O-C
12.	1043.7	32.142	Primary amine C-N stretch	C-N
13.	939.3	87.721	Alkenes sp ² C-H bend	=C-H
14.	878.7	87.409	Alkenes sp ² C-H bend	=C-H
15.	849.8	83.588	Tri-substituted alkenes sp ² C-H bend	C-H
16.	786.5	85.048	Di-substituted aromatic sp C-H bend	C-H
17.	733.0	83.080	Mono-substituted aromatic C-H bend	C-H
C				
1.	2955.8	83.080	Alkanes sp ³ C-H stretch	C-H
2.	2926.0	60.632	Alkanes sp ³ C-H stretch	C-H
3.	2858.9	89.315	Alkanes sp ³ C-H stretch	C-H
4.	2728.4	99.307	Aldehyde C-H stretch	C-H
5.	1990.4	99.392	Cyanate C-N stretch	-C≡N
6.	1748.1	99.203	Esters C-O stretch	C=O
7.	1610.2	98.594	Conjugated alkenes C-C stretch	C=C
8.	1457.4	91.799	Aromatic ring stretch	C=C
9.	1379.1	96.026	Nitro compounds NO ₂ stretch	-N=O

Table 5 FT-IR spectra peak values of (A) petroleum ether extract of *A. occidentale*, (B) ethylacetate extract of *A. occidentale*, (C) *n*-hexane extract of *P. guajava*, (D) chloroform extract of *P. guajava*, (E) ethylacetate extract of *P. guajava*, and (F) ethylacetate extract of *T. catappa* (Continued)

S/No	Peak/band (cm ⁻¹)	%T	Functional groups/assignment	Origin
10.	1155.5	98.738	Tertiary amine C-N stretch	C-N
11.	1032.5	98.385	Primary amine C-N stretch	C-N
12.	909.5	98.686	Vinyl C-H bend	C-H
13.	805.1	98.057	Di-substituted aromatic C-H bend	C-H
14.	767.8	97.557	Di-substituted aromatic C-H bend	C-H
15.	730.6	95.929	Cis-alkenes sp ² C-H bend	C-H
16.	697.0	96.671	Cis-alkenes sp ² C-H bend	C-H
D				
1.	3615.5	97.573	Primary amines N-H stretch	N-H
2.	3391.9	94.951	Primary amines N-H stretch	N-H
3.	3056.4	96.541	Aromatic compound C-H stretch	C-H
4.	2974.4	92.265	Alkanes sp ³ C-H stretch	C-H
5.	2892.4	96.394	Alkanes sp ³ C-H stretch	C-H
6.	2307.2	99.009	Alkynes sp C-C stretch	C≡C
7.	1733.2	95.893	Aldehyde C-O stretch	C=O
8.	1636.3	98.056	Amides C-O stretch	C=O
9.	1423.8	94.187	Alkanes sp ³ C-H bend	C-H
10.	1267.3	60.465	Alkyl & aryl halides (C-F stretch)	C-F
11.	1047.4	75.523	Alkoxy C-O stretch	X-O-C
12.	879.7	89.739	Alkenes sp ² C-H bend	=C-H
13.	730.6	12.893	Para-aromatic sp ² C-H bend	C-H
E				
1.	3444.1	89.445	Alcohols O-H stretch	O-H
2.	2981.9	87.541	Alkanes sp ³ C-H stretch	C-H
3.	2907.3	95.268	Aldehydes C-H stretch	C-H
4.	2091.0	98.579	Alkynes sp C-C stretch	C≡C
5.	1889.8	98.809	Carboxylic acid C-O stretch	C=O
6.	1736.9	44.150	Aldehyde C-O stretch	C=O
7.	1446.2	87.344	Aromatic compounds C-C stretch	C=C
8.	1375.4	60.518	Nitro compounds NO ₂ stretch	-N=O
9.	1237.5	27.455	Aromatic phosphates P-O-C stretch	P-O-C
10.	1095.8	82.220	Alkoxy C-O stretch	X-O-C
11.	1043.7	33.483	Primary amine C-N stretch	C-N
12.	878.7	89.082	Aromatic phosphates P-O-C stretch	P-O-C
13.	849.8	83.047	Tri-substituted alkenes sp ² C-H bend	C-H
14.	785.5	86.047	Cis-alkenes sp ² C-H bend	C-H
15.	738.0	74.085	Cis-alkenes sp ² C-H bend	C-H
16.	704.5	83.018	Cis-alkenes sp ² C-H bend	C-H
F				
1.	3410.5	77.486	Alcohols O-H stretch	O-H
2.	2981.9	85.453	Alkanes sp ³ C-H stretch	C-H
3.	2907.3	93.016	Alkanes sp ³ C-H stretch	C-H

Table 5 FT-IR spectra peak values of (A) petroleum ether extract of *A. occidentale*, (B) ethylacetate extract of *A. occidentale*, (C) *n*-hexane extract of *P. guajava*, (D) chloroform extract of *P. guajava*, (E) ethylacetate extract of *P. guajava*, and (F) ethylacetate extract of *T. catappa* (Continued)

S/No	Peak/band (cm ⁻¹)	%T	Functional groups/assignment	Origin
4.	1725.8	56.071	Aldehyde C-O stretch	C=O
5.	1446.2	86.294	Aromatic compounds C-C stretch	C=C
6.	1375.4	62.498	Nitro compounds NO ₂ stretch	-N=O
7.	1241.2	40.429	Acyl C-O; phenol C-O stretch	C-O
8.	1088.4	77.450	Alkoxy C-O stretch	X-O-C
9.	1043.7	35.790	Alkoxy C-O stretch	X-O-C
10.	939.3	88.215	Mono-alkenes sp ² C-H bend	C-H
11.	879.7	79.321	Alkene sp ² C-H bend	C-H
12.	849.8	81.398	Tri-substituted alkenes sp ² C-H bend	C-H

%T percentage transmittance

study, using bioassay-guided approach in vitro in conjunction with the GC-MS and FT-IR systems analyses, suggested that methylated esters such as methyl tetradecanoate, hexadecanoic acid, methyl ester, pentadecanoic acid, 14-methyl-methyl ester, 9, 12-octadecadienoic acid, (Z, Z)-methyl ester, 11-octadecenoic acid, methyl ester, and 9-octadecenoic acid, methyl ester (E)- were phytochemicals from petroleum ether extract of *A. occidentale* that attenuated HbS aggregation and polymerization. The phytochemicals from fractionated leaf extracts of *A. occidentale*, *P. guajava*, and *T. catappa* that attenuated HbS aggregation and polymerization are summarized (Table 4).

There are reports on other biological activities and medicinal properties of these methylated esters. For instance, methyl tetradecanoate is a platelet aggregation inhibitor used for the prevention and treatment of cerebral injuries of hemorrhagic or ischemic origin (Nagarjunakonda et al. 2017). In addition to the potentials of hexadecanoic acid, methyl ester to attenuate HbS aggregation and polymerization, as our present findings suggest, previous studies showed that hexadecanoic acid, methyl ester from calyx of *Hibiscus sabdariffa* (green roselle) elicited membrane autolysis, inhibited biosynthesis of nitric oxide, phagocytic activity of certain cells, as well as lowered tumor necrosis factor- α (TNF α), interleukin-10 (IL-10), and prostaglandin E₂ (PGE₂) activities and induced dilation of the aorta (Cai et al. 2005; Sarkar et al. 2006; Lin et al. 2009). Methyl stearate is an anti-helminthic, anti-fungal, and anti-nociceptive agent as well as a potent γ -amino butyric acid (GABA) aminotransferase inhibitor, lipid metabolism regulator, gastrin inhibitor, and exhibits antioxidant activity (Pinto et al. 2017; Adnan et al. 2019). Other notable biological activities and medicinal properties of few other phytochemicals, as our present findings suggest, that attenuated HbS aggregation and polymerization are summarized elsewhere: viz. pentadecanoic acid, 14-methyl-, methyl

ester (antioxidant) (Vijisarl and Arumugam 2014), phthalates (antibacterial) (Khatiwora et al. 2012), isothiocyanates (antimicrobial) (Dias et al. 2014), and arachidyl alcohols (Garaniya and Bapodra 2014).

Conclusion

The fractionated leaf extracts of *A. occidentale*, *P. guajava*, and *T. catappa* that exhibited comparatively high potency to attenuate HbS aggregation and polymerization were as follows: petroleum ether extract of *A. occidentale*, ethylacetate extract of *A. occidentale*, as well as *n*-hexane extract of *P. guajava*. Other fractionated leaf extracts that attenuated HbS aggregation and polymerization were chloroform extract of *P. guajava*, ethylacetate extract of *P. guajava*, and ethylacetate extract of *T. catappa*. The fractionated leaf extracts of *A. occidentale*, *P. guajava*, and *T. catappa* exhibited differential capacities to impede HbS aggregation and polymerization in the order of *n*-hexane extract of *P. guajava* > ethylacetate extract of *A. occidentale* > ethylacetate extract of *P. guajava* > ethylacetate extract of *T. catappa* > petroleum ether extract of *A. occidentale*.

The identification, quantitation, and characterization methods using GC-MS in conjunction with FT-IR and UV-visible systems protocols revealed combinations of 53 phytochemicals from the fractionated leaf extracts of *A. occidentale*, *P. guajava*, and *T. catappa* as molecular species that impeded HbS aggregation and polymerization in vitro. In general terms, the phytochemicals from the fractionated leaf extracts that attenuated HbS aggregation and polymerization include the aliphatic hydrocarbons, methylated esters, methylated long-chain and short-chain fatty acids, volatile alkanes, short-chain aliphatic alcohols, D-erythro-sphinganine, aromatic derivatives, cycloalkanes, phthalates, isothiocyanates, aminated sugars, cyclo-alcohols, arachidyl alcohols, and nitro-compounds.

The effectiveness of GC-MS, FT-IR, and UV-visible systems protocols notwithstanding, identification of unknown molecular species largely relied on comparison with known molecules from a database/library and established chromatogram and fingerprints patterns. Consequently, the use of these methods for the classification of phytochemicals into functional and structural groups comes with few drawbacks and challenges. Therefore, it is recommended that further investigations should be carried out for such exercise. Additionally, in order to confirm the specific identities of the phytochemicals that attenuated HbS aggregation and polymerization, it is recommended that another study on isolation and purification of the phytochemicals, suggested in the present study, should be applied in further HbS polymerization studies *in vitro* as well as the use transgenic sickle animal model.

Abbreviations

GC-MS: Gas chromatography-mass spectrometry; FT-IR: Fourier transform-infrared spectrometry; UV-visible: Ultraviolet-visible spectroscopy; Poly-dHbS-M: Polymerization of deoxygenated sickle hemoglobin molecules; PBS: Phosphate-buffered saline; NaCl: Sodium chloride; Na₂S₂O₅: Sodium metabisulfite; RCP%: Relative cumulative polymerization index; HbS: Sickle hemoglobin; HbSS: Homozygous sickle hemoglobin; dHbS-M: Deoxygenated sickle hemoglobin molecules; SCD: Sickle cell disease; HbF: Fetal hemoglobin; Na₂HPO₄·2H₂O: Disodium hydrogen phosphate dihydrate; NaH₂PO₄·2H₂O: Sodium dihydrogen phosphate dihydrate

Acknowledgements

The authors are grateful for the technical assistance offered by Mr. F.C. Emengaha, Chief Academic Technologist, Department of Medical Biochemistry, College of Medicine and Mr. C.O. Kabiri, Senior Laboratory Technologist, Department of Biochemistry, Faculty of Science, Imo State University, Owerri. Mr. Franklyn O. Ohiagu efforts are highly appreciated.

Authors' contributions

PCC conceived and designed the research and supervised the laboratory work. PCC prepared the manuscript. PCC/RCE/ABC-A analyzed the data. PCC/RCE/ABC-A collected the plant samples and carried out the laboratory work. PCC supervised the laboratory work. All authors have approved the manuscript in the present form and gave the permission to submit the manuscript for publication.

Funding

This work was supported by Imo State University, Owerri, and research grant offered by the Tertiary Education Trust Fund (TETFund) Research Based Interventions of Nigerian Universities. Imo State University, Owerri, provided the laboratory space and infrastructures. TETFund provided the financial resources for purchase of laboratory chemicals/reagents and instruments as well as expenses pertaining to transportation and travels. Grant Number: TETFUND/DRSS/UNIV/OWERRI/2015/5RP VOL 1 (7).

Availability of data and materials

All the data generated and analyzed during the study are included in the main manuscript.

Ethics approval and consent to participate

The collection of the blood samples was in accordance with the ethical principles that have their origins in the October 2008 Declaration of Helsinki. The present study was approved by the Ethical Committee for Research, Department of Biochemistry, Imo State University, Owerri, Nigeria. Ethics Approval Number: ODVC/REN/544/19. Written consent was obtained whereby all the participants filled and signed an Informed Consent Form.

Consent for publication

Not applicable.

Competing interests

The authors declare that they have no competing interests.

Received: 14 July 2020 Accepted: 6 August 2020

Published online: 17 August 2020

References

- Abdulmalik O, Safo MK, Chen Q, Yang J, Brugnara C, Ohene-Frempong K (2005) 5-hydroxymethyl-2-furfural modifies intracellular sickle haemoglobin and inhibits sickling red blood cells. *Br J Haematol* 128:552–561
- Adachi KS, Konitzer P, Paulraj CG, Surre S (1994) Role of Leu-β88 in the hydrophobic acceptor pocket for Val-β6 during hemoglobin S polymerization. *J Biol Chem* 269(26):17477–17480
- Adewoyin AS, Alagbe AE, Adedokun BO, Idubor NT (2015) Knowledge, attitude and control practices of sickle cell disease among youth corps members in Benin City, Nigeria. *Ann Ibadan Postgrad Med* 13(2):100–107
- Adnan M, Chy NU, Kamal ATM, Azad MOK, Paul A, et al. (2019) Investigation of the biological activities and characterization of bioactive constituents of *Ophiorrhiza rugosa* var. *prostrata* (D.Don) and *Mondal* leaves through *in vivo*, *in vitro*, and *in silico* approaches. *Mole* 24:1367. 24 pages.
- Bain B, Bates I, Laffan M (2012) *Dacie and Lewis practical haematology*. Amsterdam. The Netherlands, Elsevier Health Sciences
- Bianchi N, Zuccato C, Lampronti I, Borgatti M, Gambari R (2009) Fetal hemoglobin inducers from the natural world: a novel approach for identification of drugs for the treatment of β-thalassemia and sickle-cell anemia. *Compl Altern Med* 6(2):141–151
- Cai P, Kaphalia BS, Ansari GA (2005) Methyl palmitate: inhibitor of phagocytosis in primary rat Kupffer cells. *Toxicol* 210:197–204
- Chang H, Ewert SM, Nagel RL (1983) Identification of 2-imidazolines as anti-sickling agents. *Am Soc Pharmacol Exp Ther* 23(3):731–734
- Charache S, Terrin M, Moore R, Dover G, Barton F, Eckert S (1995) The effect of hydroxyurea on the frequency of painful crises in sickle cell anemia. *N Engl J Med* 332:1317–1322
- Chikezie PC (2011) Sodium metabisulphite induced polymerization of sickle cell haemoglobin (HbS) incubated in extracts of three medicinal plants (*Anacardium occidentale*, *Psidium guajava* and *Terminalia catappa*). *Pharmacogn Mag* 7(26):126–132
- Chikezie PC, Akuwudike AR, Chikezie CM (2013) Polymerization studies of sickle cell hemoglobin incubated in aqueous leaf extract of *Nicotiana tabacum* product. *Res J Med Plant* 7(2):92–99
- Chikezie PC, Chikezie CM, Amaragbulem PI (2010) Effect of antimalarial drugs on polymerization of sickle cell hemoglobin (HbS). *Turk J Biochem* 35(1):41–44
- Chikezie PC, Ibegbulem CO, Mbagwu FN (2015) Bioactive principles from medicinal plants. *Res J Phytochem* 9(3):88–115
- Chikezie PC, Ojiako AO (2013) Cyanide and aflatoxin loads of processed Cassava (*Manihot esculenta*) tubers (Garri) in Njaba, Imo State, Nigeria. *Toxicol Int* 20(3):261–267
- Chikezie PC, Uwakwe AA (2011) Membrane stability of sickle erythrocytes incubated in extracts of three medicinal plants: *Anacardium occidentale*, *Psidium guajava* and *Terminalia catappa*. *Pharmacogn Mag* 7(26):121–125
- Cokic VP, Smith RD, Beleslin-Cokic BB, Njoroge JM, Miller JL et al (2003) Hydroxyurea induces fetal hemoglobin by the nitric oxide-dependent activation of soluble guanylyl cyclase. *J Clin Invest* 111(2):231–239
- Cyril-Olutayo MC, Agbedahunsi JM, Akinola NO (2019) Studies on the effect of a nutritious vegetable, *Telfairia occidentalis*, on HbSS blood. *J Tradit Compl Med* 9:156–162
- Dash BP, Archana Y, Satapathy N, Naik SK (2013) Search for antisickling agents from plants. *Pharmacogn Rev* 7(13):53–60
- Diallo D, Tchernia G (2002) Sickle cell disease in Africa. *Curr Opin Hematol* 9(2): 111–116
- Dias C, Aires A, Saavedra MJ (2014) Antimicrobial activity of isothiocyanates from cruciferous plants against methicillin-resistant *Staphylococcus aureus* (MRSA). *Int J Mol Sci* 15:19552–19561
- Ding F, Liu W, Sun Y, Yang X-L, Sun Y et al (2012) Analysis of conjugation of chloramphenicol and hemoglobin by fluorescence, circular dichroism and molecular modeling. *J Mol Struct* 1007:81–87
- Eaton WA, Bunn HF (2017) Treating sickle cell disease by targeting HbS polymerization. *Blood* 129(20):2719–2726

- Eaton WA, Hofrichter J (1987) Hemoglobin S gelation and sickle cell disease. *Blood* 70:1245–1266
- Eliot R, Davies M, Hamse DJ (2006) Dermatomyositis-like eruption with long-term hydrourae. *Br J Dermatol* 17:56–60
- Ezekwe SA, Chikezie PC (2017) GC-MS analysis of aqueous extract of unripe fruit of *Carica papaya*. *J Nutr Food Sci* 7(3):5 pages.
- Ferrone FA, Ivanova M, Jasuja R (2002) Heterogeneous nucleation and crowding in sickle hemoglobin: An analytic approach. *Biophys J* 82(1):399–406
- Frenette PS, Atweh GF (2007) Sickle cell disease: Old discoveries, new concepts, and future promise. *J Clin Invest* 117:850–858
- Garaniya N, Bapodra A (2014) Ethnobotanical and phytopharmacological potential of *Abrus precatorius* L.: A review. *Asian Pac J Trop Biomed* 4(1):S27–S34
- Grosse SD, Odame I, Atrash HK, Amendah DD, Piel FB, Williams TN (2011) Sickle cell disease in Africa: A neglected cause of early childhood mortality. *Am J Prev Med* 41(6S4):S398–S405.
- Hamdani S, Joly D, Carpentier R, Tajmir-Riahi HA (2009) The effect of methylamine on the solution structures of human and bovine serum albumins. *J Mol Struct* 936(1–3):80–86
- Hemavathy A, Shanthy P, Sowndharya C, Thiripura SS, Priyadarshini K (2019) Extraction and isolation of bioactive compounds from a therapeutic medicinal plant - *Wrightia tinctoria* (Roxb.). *R. Br Int J Pharmacogn Phytochem Res* 11(3):199–204
- Ighodaro OM, Akinloye OA, Ugbara RN, Omotainse SO, Faokunla O (2016) FT-IR analysis of *Sapium ellipticum* (Hochst) pax ethanol leaf extract and its inhibitory effects on pancreatic α -amylase and intestinal α -glucosidase activities *in vitro*. *Egypt J Basic Appl Sci* 3(4):343–349
- Imaga NA (2013) Phytomedicines and nutraceuticals: alternative therapeutics for sickle cell anemia. *Sci World J* 2013: Article ID 269659, 12 pages.
- Jana S, Strader MB, Meng F, Hicks W, Kassa T et al (2018) Hemoglobin oxidation-dependent reactions promote interactions with band 3 and oxidative changes in sickle cell-derived microparticles. *JCI Insight* 3(21):e120451
- Kapoor S, Little JA, Pecker LH (2018) Advances in the treatment of sickle cell disease. *Mayo Clin Proc* 93(12):1810–1824
- Karayil S, Chandran KPS, Sudeesh PS, Veralia K (2014) Isolation and Structural elucidation of novel bioactive molecule-Coumarin from traditionally used medicinal plant-*Ceropegia juncea* (Roxb.). *IOSR. J Pharm Biol Sci* 9:19–22
- Kark JA, Kale MP, Tarassoff PG, Woods M, Lessin LS (1988) Inhibition of erythrocyte sickling *in vitro* by pyridoxal. *J Clin Invest* 62:888–891
- Kassa T, Wood F, Strader MB, Alayash AI (2019) Antisickling drugs targeting β Cys93 reduces iron oxidation and oxidative changes in sickle cell hemoglobin. *Front Physiol* 10(931):1–12
- Khatiwora E, Adsul VB, Kulkarni M, Deshpande NR, Kashalkar RV (2012) Antibacterial activity of Dibutyl phthalate: a secondary metabolite isolated from *Ipomoea carnea* stem. *J Pharm Res* 5(1):150–152
- Lin HW, Liu CZ, Cao D, Chen PY, Chen MF et al (2009) Endogenous methyl palmitate modulates nicotinic receptor-mediated transmission in the superior cervical ganglion. *Proc Nat Acad Sci, USA* 105:19526–19531
- Makani J, Ofori-Acquah SF, Nnodu O, Wonkam A, Ohene-Frempong K (2013) Sickle cell disease: new opportunities and challenges in Africa. *Sci World J* Article ID 193252:16 pages
- Manning JM, Acharya AS (1984) The mechanism of action of two antisickling agents: Sodium cyanate and glyceraldehyde. *Am J Pediatr Hematol Oncol* 6: 51–54
- Martins DW (1983) Structure and function of a protein-haemoglobin. In: Harper's Review of Biochemistry. Martin DW, Mayes PA, Rodwell VW. (Editors). 9th Edition. Lange Medical Publications. California. pp. 40–50.
- Mburu FW, Swaleh S, Njue W (2012) Potential toxic levels of cyanide in cassava (*Manihot esculenta* Crantz) grown in Kenya. *Afr J Food Sci* 6:416–420
- Mohd FB, Abdul R, Pin KY, Zamree MS, Luqman CA et al (2012) The effects of varying solvent polarity on extraction yield of *Orthosiphon stamineus* leaves. *J Appl Sci*. 12:1207–1210
- Mousavi B, Tafvizi F, Zaker BS (2018) Green synthesis of silver nanoparticles using *Artemisia turcomanica* leaf extract and the study of anti-cancer effect and apoptosis induction on gastric cancer cell line. *Artif Cell Nanomed Biotechnol* 46(1):499–510
- Mulumba LL, Wilson L (2015) Sickle cell disease among children in Africa: An integrative literature review and global recommendations. *Int J Afr Nursing Sci* 3:56–64
- Nagarjunakonda S, Amalakanti S, Dhishana SR, Ramaiah M, Rajanala L (2017) GC-MS analysis of Indrakeeladi native medicine used in the treatment of stroke. *Pharmacogn J* 9(1):102–106
- Nurain IO, Bewaji CO, Johnson JS, Davenport RD, Zhang Y (2017) Potential of three ethnomedicinal plants as antisickling agents. *Mol Pharm* 14(1):172–182
- Oder E, Safo MK, Abdulmalik O, Kato GJ, Discovery D (2016) New developments in anti-sickling agents: Can drugs directly prevent the polymerization of sickle haemoglobin *in vivo*? *Br J Haematol* 175(1):24–30
- Ojiako AO, Chikezie PC, Ogbuji CA (2015) Histopathological studies of renal and hepatic tissues of hyperglycemic rats administered traditional herbal formulations. *Int J Green Pharm* 9(3):184–191
- Okoye TC, Akah PA, Okoli CO, Ezike AC, Mbaaji FN (2010) Antimicrobial and antispasmodic activity of leaf extract and fractions of *Stachytarpheta cayennensis*. *Asian Pac J Trop Med* 2010:189–192
- Okpuzor J, Adebesein O, Ogbunugafor H, Amadi I (2008) The potential of medicinal plants in sickle cell disease control: A review. *Int J Biomed Health Sci* 4(2):47–55
- Oyewole O, Malomo S, Adebayo J (2008) Comparative studies on antisickling properties of thiocyanate, tellurite and hydroxyurea. *Pak J Med Sci* 24(1):18
- Park S, Hayes BL, Marankan F, Mulhearn DC, Wanna L et al (2003) Regioselective covalent modification of hemoglobin in search of antisickling agents. *J Med Chem* 46:936–953
- Pauline N, Cabral BNP, Anatole PC, Jocelyne AMV, Bruno M, Jeanne NY (2013) The *in vitro* antisickling and antioxidant effects of aqueous extracts *Zanthoxylum heitzii* on sickle cell disorder. *BMC Compl Altern Med* 13(1):162
- Piccin A, Murphy C, Eakins E, Rondinelli MB, Daves M, Vecchiato C (2019) Insights into the complex pathophysiology of sickle cell anaemia and possible treatment. *Eur J Haematol* 2019:1–12
- Pinto MEA, Araújo SG, Morais MI, Sá NP, Lima CM (2017) Antifungal and antioxidant activity of fatty acid methyl esters from vegetable oils. *Ann Braz Acad Sci* 89(3):1671–1181
- Rašković A, Pavlović N, Kvirgić M, Sudji J, Mitić G, Čapo I (2015) Effects of pharmaceutical formulations containing thyme on carbon tetrachloride-induced liver injury in rats. *BMC Compl Altern Med* 15:442
- Rotter MA, Kwong S, Briehl RW, Ferrone FA (2005) Heterogeneous nucleation in sickle hemoglobin: Experimental validation of a structural mechanism. *Biophys J* 89:2677–2684
- Safo MK, Kato GJ (2014) Therapeutic strategies to alter the oxygen affinity of sickle haemoglobin. *Haematol Oncol Clin N Am* 28:17
- Sampaio KL, Garruti DS, Franco MRB, Janzanti NS, Da Silva MAP (2011) Aroma volatiles recovered in the water phase of cashew apple (*Anacardium occidentale* L.) juice during concentration. *J Sci Food Agric* 91:1801–1809
- Sarkar S, Khan MF, Kaphalia BS, Ansari GA (2006) Methyl palmitate inhibits lipopolysaccharide-stimulated phagocytic activity of rat peritoneal macrophages. *J Biochem Mol Toxicol* 20:302–308
- Sasidharan S, Chen Y, Saravanan D, Sundram KM, Yoga LL (2011) Extraction, isolation and characterization of bioactive compounds from plants' extracts. *Afr J Tradit Compl Altern Med* 8:1–10
- Saxena M, Saxena J, Nema R, Singh D, Gupta A (2013) Phytochemistry of medicinal plants. *J Pharmacogn Phytochem* 1(6):168–170
- Semwa P, Painuli S (2019) Antioxidant, antimicrobial, and GC-MS profiling of *Saussurea obvallata* (Brahma Kamal) from Uttarakhand Himalaya. *Clin Phytosci* 5:12, 11 pages
- Setty BNY, Kulkarni S, Rao AK, Stuart MJ (2000) Fetal hemoglobin in sickle cell disease: relationship to erythrocyte phosphatidylserine exposure and coagulation activation. *Blood* 96(3):1119–1124
- Stallworth JR, Jerrell JM, Tripathi A (2010) Cost-effectiveness of hydroxyurea in reducing the frequency of pain episodes and hospitalization in pediatric sickle cell disease. *Am J Haematol* 85(10):795–797
- Syed MM, Doshi PJ, Dhavale DD, Doshi JB, Kate SL et al (2019) Potential of isoquercitrin as antisickling agent: a multi-spectroscopic, thermophoresis and molecular modeling approach. *J Biomole Strut Dyn* 2019:20 pages. <https://doi.org/10.1080/07391102.2019.1645735>
- Tsakiris S, Giannoulia-Karantana A, Simintzi I, Schulpis KH (2005) The effect of aspartame metabolites on human erythrocyte membrane acetylcholinesterase activity. *Pharmacol Res* 53:1–5
- Uwakwe AA, Nwaoguikpe RN (2008) *In vitro* antisickling effects of *Xylopia aethiopica* and *Monodora myristica*. *J Med Plant Res* 2:119–124
- Uzunova VV, Pan W, Galkin O, Vekilov PG (2010) Free heme and the polymerization of sickle cell hemoglobin. *Biophys J* 99:1976–1985
- Vekilov PG (2007) Sickle-cell haemoglobin polymerization: is it the primary pathogenic event of sickle cell anaemia? *Br J Haematol* 139(2):173–184
- Vijisara ED, Arumugam S (2014) GC-MS analysis of bioactive constituents of *Indigofera suffruticosa* leaves. *J Chem Pharmaceut Res* 6(8):294–300

- Weatherall DJ, Akinyanju O, Fucharoen S, Olivieri NF, Musgrove P (2006) Inherited disorders of hemoglobin. In: *Disease Control Priorities in Developing Countries*. D. Editor. Oxford University Press. New York, USA, Jamison, pp 663–680
- World Health Organization Regional Office for Africa. Sickle-cell disease: a strategy for the WHO African Region. Report of the Regional Director. Geneva, Switzerland: WHO, 22 June 2010. AFR/RC60/8.
- Xu ASL, Labotka RJ, London RE (1999) Acetylation of human hemoglobin by methyl acetylphosphate: Evidence of broad regio-selectivity revealed by NMR studies. *J Biol Chem* 274:26629–26632
- Yamamoto A, Saito N, Yamauchi Y, Takeda M, Ueki S, Itoga M et al (2014) Flow cytometric analysis of red blood cell osmotic fragility. *J Lab Auto* 19(5):483–487

Publisher's Note

Springer Nature remains neutral with regard to jurisdictional claims in published maps and institutional affiliations.

Submit your manuscript to a SpringerOpen[®] journal and benefit from:

- ▶ Convenient online submission
- ▶ Rigorous peer review
- ▶ Open access: articles freely available online
- ▶ High visibility within the field
- ▶ Retaining the copyright to your article

Submit your next manuscript at ▶ [springeropen.com](https://www.springeropen.com)
